GEOLOGIJA *61/1*, 49-71, Ljubljana 2018
© Author(s) 2018. CC Atribution 4.0 License

https://doi.org/10.5474/geologija.2018.004

Lower Jurassic succession at the site of potential Roman quarry Staje near Ig (central Slovenia)

Spodnjejurske plasti na območju morebitnega rimskega kamnoloma Staje pri Igu

Boštjan ROŽIČ[1], Luka GALE[1,2], Rok BRAJKOVIĆ[2], Tomislav POPIT[1] & Petra ŽVAB ROŽIČ[1]

[1]University of Ljubljana, Faculty of Natural Sciences and Engineering, Department for Geology, Privoz 11, SI-1000 Ljubljana, Slovenia;
[2]Geological Survey of Slovenia, Dimičeva ul. 14, SI-1000 Ljubljana, Slovenia
e-mail: bostjan.rozic@ntf.uni-lj.si, luka.gale@ntf-lj.si, rok.brajkovic@geo-zs.si, tomi.popit@ntf.uni-lj.si, petra.zvab@ntf.uni-lj.si.

Prejeto / Received 22. 3. 2018; Sprejeto / Accepted 19. 6. 2018; Objavljeno na spletu / Published online 20. 7. 2018

Key words: Lower Jurassic, Sinemurian, Dinaric Carbonate Platform, neptunian dyke, microfacies, Roman quarry

Ključne besede: spodnja jura, sinemurij, Dinarska karbonatna platfroma, neptunski dajk, mikrofacies, rimski kamnolom

Abstract

Several locations along the southern margin of the Ljubljana Moor have been proposed as sites of antique Roman quarries, but except for the site in the village of Podpeč, no detailed sedimentological investigations, which would reveal the spectrum of available natural stone, have yet been made. This paper presents a section logged at the potential Roman quarry from the small valley southeast of the village of Staje near Ig. The section is composed of Sinemurian strata dominated by micritic limestone with dissolution voids and bioclastic limestone, mostly wackestone with mollusks. Other facies are rare aggregate-grain/ooidal calcarenite, lumachella, limestone microbreccia, and stromatolitic limestone. Altogether, 21 microfacies types are described. Facies association points to sedimentation in restricted and open marine lagoon repeatedly subjected to emersion, rarely high-energy conditions or events. Previously unrecorded on the Dinaric Carbonate Platform in this area are neptunian dykes that occur as fractures partially filled by calcite cement and partially by intra/bioclastic packstone containing upper Jurassic microfossils. These could potentially serve as a diagnostic feature for recognizing artefacts made from stone quarried at Staje.

Izvleček

Do sedaj je bilo vzdolž južnih obronkov Ljubljanskega barja predlaganih nekaj lokacij kot domnevno rimskih kamnolomov, vendar nobena izmed teh, razen Podpeči, ni bila detajlno sedimentološko raziskana. Spekter dostopnega naravnega kamna tako ostaja dokaj slabo poznan. V tem prispevku predstavljamo profil, ki je bil posnet na območju morebitnega rimskega kamnoloma v majhni dolini jugovzhodno od vasi Staje pri Igu. Profil sestavljajo spodnjejurske, natančneje sinemurijske plasti, v katerih prevladujejo mikritni apnenci z dvema generacijama korozijskih votlinic in bioklastični apnenci, večinoma tipa wackestone z mehkužci. Ostali faciesi so redki kalkareniti z agregatnimi zrni ali ooidi, lumakela in apnenčeva mikrobreča. V raziskanem zaporedju izdvajamo 21 mikrofaciesnih tipov. Faciesna združba kaže na sedimentacijo v zaprti in občasno odprtomorski laguni, ki je bila podvržena ponavljajočim se okopnitvam, redko pa tudi višjeenergijskim razmeram ali dogodkom. Raziskane plasti ustrezajo predhodno opisanemu spodnjejurskemu zaporedju širšega območja, ki kaže postopno odpiranje iz hettangijskega medplimskega sedimentacijskega okolja v pliensbachijsko razgibano laguno. Pomemben element profila Staje so tudi neptunski dajki, ki do sedaj niso bili poznani v kamninah Dinarske karbonatne platfrome tega območja. Pojavljajo se v obliki razpok, zapolnjenih deloma s kalcitnim cementom, deloma pa s sedimentom tipa intra/bioklastični packstone, ki vsebuje zgornjejurske fosile. Le ti bi kot specifična značilnost lahko služili pri razločevanju artefaktov narejenih iz naravnega kamna pridobljenega iz območja Staj.

Introduction

The large alluvial fan of the Iška River at the southern outskirts of the Ljubljana Moor has been populated since pre-history (Velušček, 2004, 2010). During the first centuries AD the settlements from the Iška alluvial fan supplied the evolving colony of Emona (Šašel Kos, 2009) and left rich archaeological evidence, including numerous sepulchral monuments (roman tombstones) (Šašel, 1959; Ragolič, 2016; Veranič & Repanšek, 2016).

At Marof near Ig, the archaeological site was discovered in the year 2014, which included a pit with stone monuments from the Roman period (Ragolič, 2016). The majority of these monuments are made of limestone, for which a local origin has been presumed (Žvab Rožič et al., 2016). Proof of Roman use of natural stone comes to us from depictions on stone monuments (stelae), which indicate that the Roman-era inhabitants of the Ig area were involved in quarrying, forestry, and metalworking (Šašel, 1959). Ramovš (in Šašel Kos, 1997) mentions four locations of possible quarries from the Roman period along the southern outskirts of the Ljubljana Moor: Sveta Ana, Podpeč, Staje and Skopačnik (listed moving from west to east). The only proven roman quarry is that known in the village of Podpeč (Ramovš, 2000; Djurić & Rižnar, 2017), because during the archaeological excavations by B. Djurić in 2017 remains of Roman-age architecture were found inside the quarry (Djurić, pers.comm.). In this locality grey, dark grey and almost black Pliensbachian limestone with abundant ooids and bioclasts is exposed (Buser & Debeljek, 1995; Gale, 2014, 2015; Kramar et al., 2015). However, as pointed out already by Žvab Rožič and co-workers (2016), facies of analysed artefacts from Marof differ from the Podpeč limestone. Nor does it correspond to the Lower Triassic limestone of the potential ancient quarry near the Skopačnik farm that was described by Mušič (1990). Until now, there was no detailed lithological data from the other two sites (Sveta Ana and Staje) of potential ancient quarries.

This paper is the result of geological research of the Lower Jurassic succession from the village of Staje, i.e. the proposed site of the Roman quarry that was located closest to the above-mentioned Marof archeological site (cf. Ramovš - in Šašel Kos, 1997). We provide a detailed sedimentologic and biostratigraphic description of the limestone succession from the Staje section from the site where the ancient quarry was most likely situated. This data will serve as the basis for comparison with stone artefacts recovered at Marof and other archaeological sites located close by.

Geological setting

The studied succession is located on the northern edge of the Krim-Mokrec Mountain Range and structurally belongs to the Hrušica Nappe of the External Dinarides (fig. 1) (Placer, 1999; 2008). The main structures of the area are NW-SE oriented strike-slip faults (Buser et al., 1967; Buser, 1968). During the Mesozoic this area belonged to the northern part of the Dinaric (Adriatic) Carbonate Platform; thus, Upper Triassic to Middle Jurassic carbonates prevail (fig. 1). The Upper Triassic begins with a thin succession of coarse-crystalline ("cordevolian") dolomite, part of which could be Middle Triassic in age (Celarc, 2004, 2008). It is followed by a thick peritidal Norian-Rhaetian Main Dolomite Formation. The Lower Jurassic part is dominated by micritic and bioclastic limestones that alternate with ooidal limestone. In the Pliensbachian part of this succession, lithiotid bivalves occur (Buser & Debeljak, 1995; Debeljak & Buser, 1997; Gale 2014, 2015), whereas the Toarcian part is marked by thin-bedded micritic limestone (Dozet, 2009). The Middle Jurassic is composed almost exclusively of ooidal limestone (Miler & Pavšič, 2008). Jurassic limestones are often replaced by dolomite (Buser et al., 1967, Buser, 1968; Miler & Pavšič, 2008). In addition to the described carbonates, Paleozoic clastics and Early Triassic carbonate-clastic succession outcrops to the east of the studied area (Buser, 1968; Mušič, 1990). To the north the described units are covered by Quaternary alluvial fan coarse-clastic sediments, which further north interfinger with lacustrine and marsh deposits (Buser et al., 1967, Buser, 1968).

Methods

The micro-location of the potential Roman quarry was determined using a combination of fieldwork observations and analysis of the digital elevation model based on detailed 1 × 1m Lidar data. In the selected area a detailed sedimentological section (almost 40 m at 1:50 scale) was logged and densely sampled. Logging included measurements of structural elements (orientation and dip of fractures, veins, neptunian dykes). A total of 58 samples were selected; from these, 62 thin-sections were made for microfacies and biostratigraphic analysis. Names of the sample correspond to the stratimetric position of the logged section (sample 7.1 was taken at the 7.1th m of the section). The size of the ooids and aggregate grains, and the number of ooid laminae were measured in at least 30 grains in each thin-section dominated by these grains.

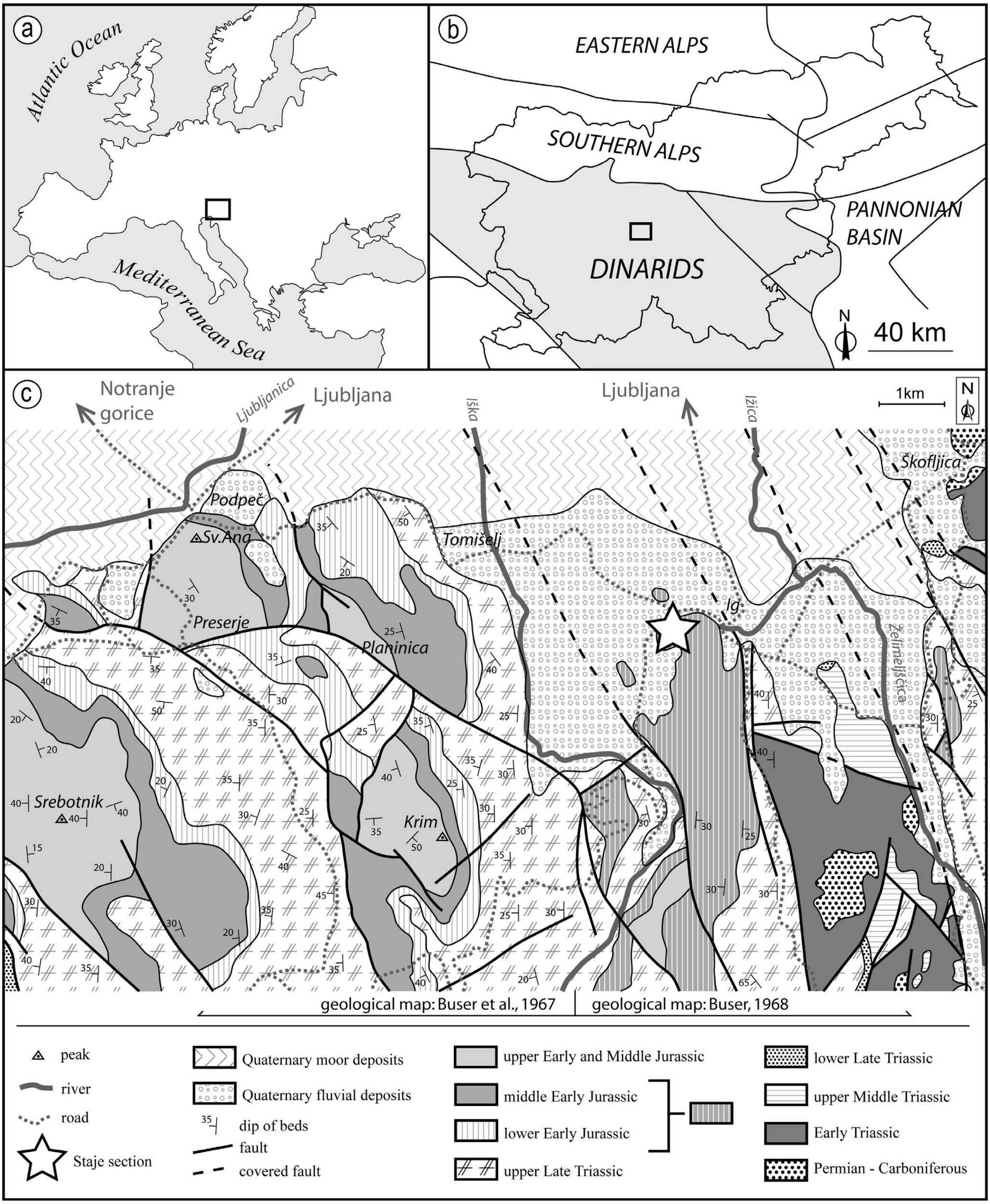

Fig. 1. a) Location of the studied section (boxed area is enlarged to the right). b) Macrotectonic subdivision of Slovenia (after Placer, 1999) with marked position of geological map below. c) Simplified geological map of the southern outskirts of the Ljubljana Moor (compiled from Buser et al., 1967 and Buser, 1968). The star marks the location of the studied section.

Micro-location of the potential Roman quarry

The hilly area south of the village of Staje is composed of Lower Jurassic limestone and subordinate dolomite (fig. 2). This karstic terrain is dominated by dolines and passes into the relatively flat Iška River alluvial fan. On the transitional belt (including the area of Staje and other villages) between the hills and flatland, the gravel-sand sediments also cover geomorphological depressions within outcropping base-rock, such as valleys and larger dolines. Anthropogenic al-

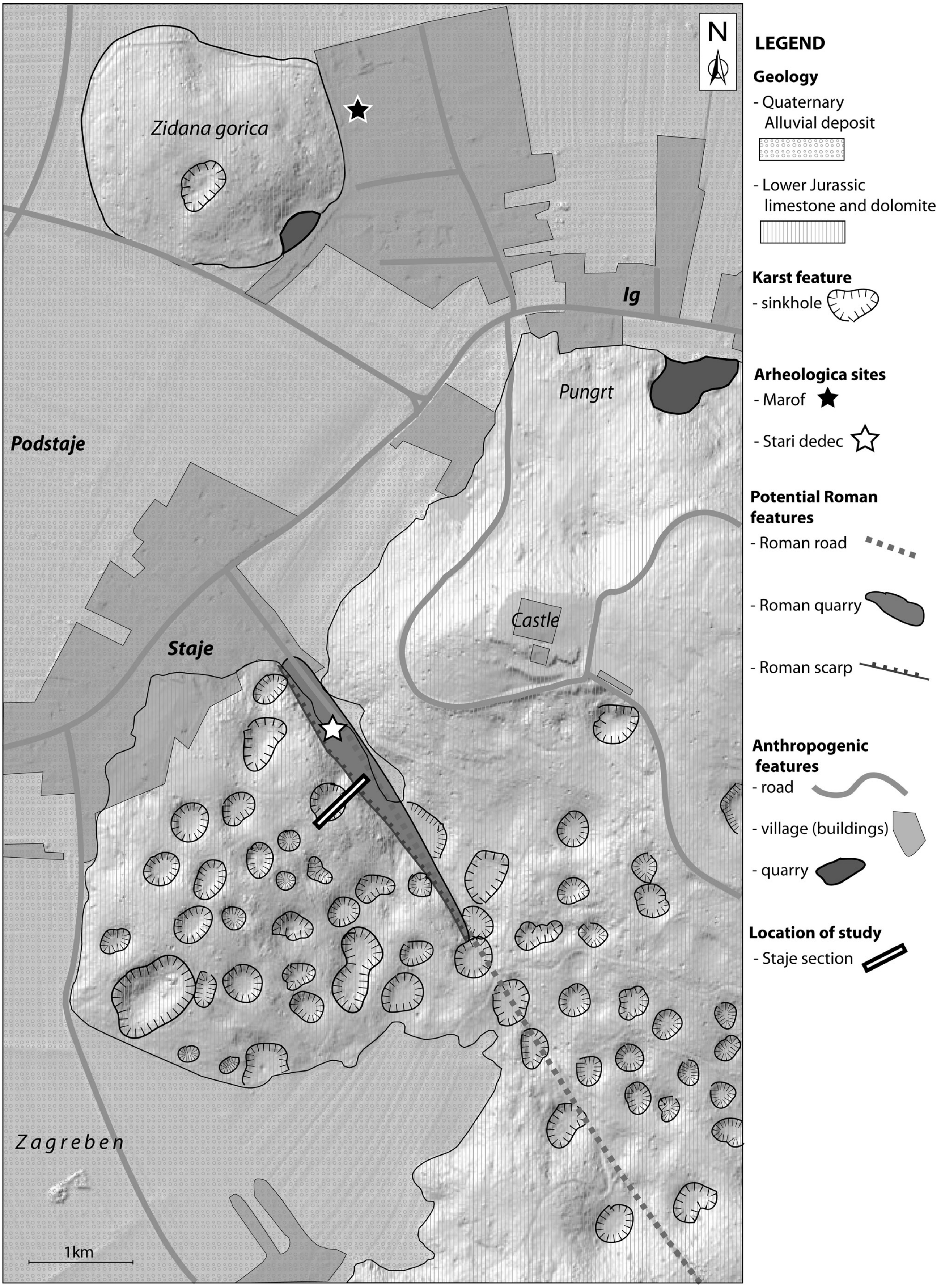

Fig. 2. Geomorphological map of the area of Staje and Marof with marked positions of the logged section (potential roman quarry), "Stari dedec" Roman monument and Marof arheological site.

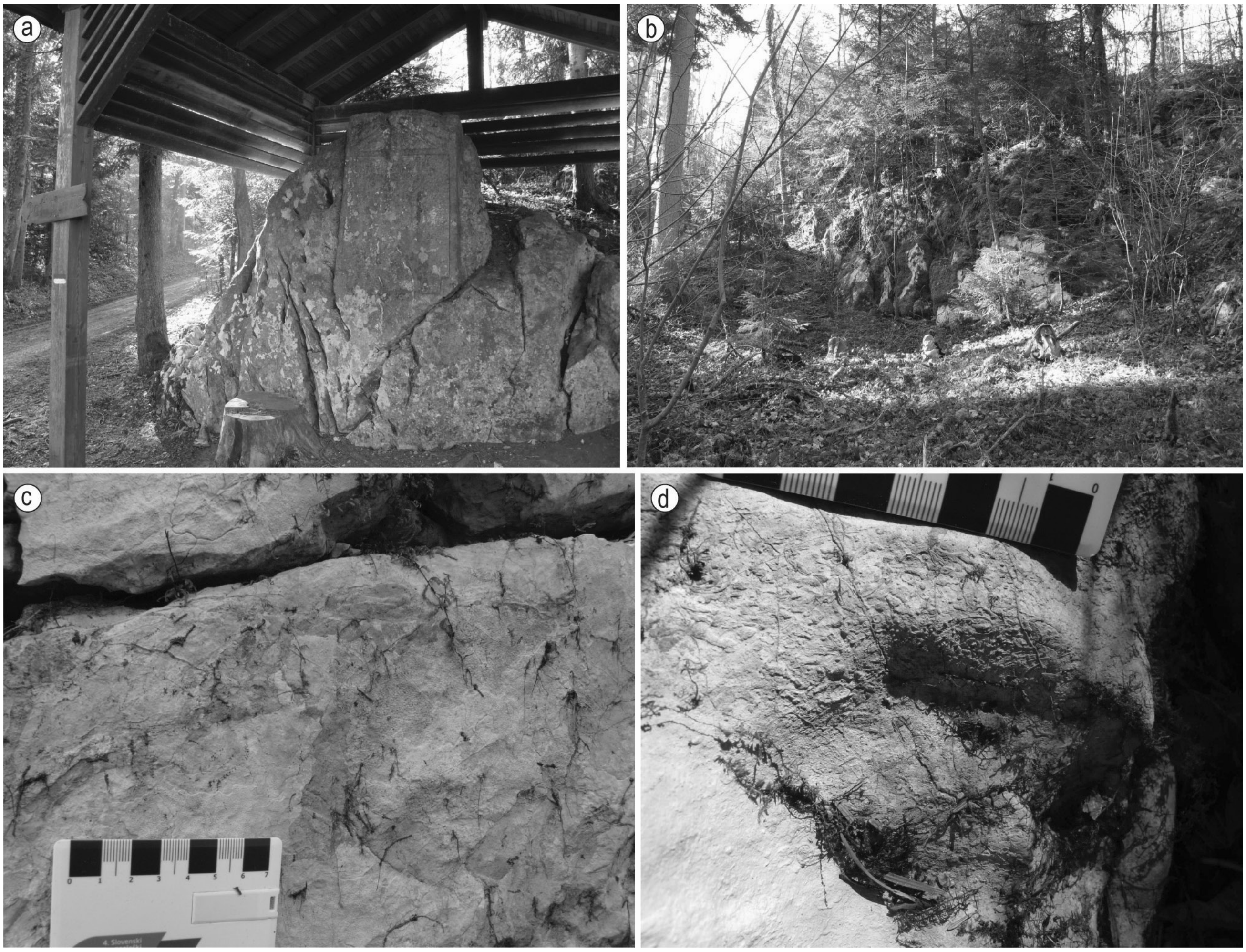

Fig. 3. a) "Stari dedec" Roman stela carved into the massive limestone outcrop at the entrance to the valley with potential roman quarry. b) Limestone escarpment at SW bank of the valley that could be of anthropogenic origin. c) Reddish sediment infill of large dissolution void (5. m of the section). d) Bioclastic rudstone deposited above erosional surface (just above 20. m of the section).

terations of the bedrock can be recognized in the area of the villages of Staje and Ig, on the Pungrt hill, where the Ig Castle is situated, and at the SW flank of the flat valley that runs from the village of Staje in the SE direction (figs. 3a, b). The latter shows a straight escarpment, which is in stark contrast to the NE flank of the same valley, which is defined by soft karstic lines (some are probably dolines filled by gravel and sand deposits). The escarpment on the SW flank of valley is a subvertical rock-wall stretching up to 6 m in height. Fractures run parallel to the massive wall surface, whereas rock debris is accumulated at the base of the wall.

As already mentioned by Vuga (2000a, b), this might be the site of ancient extraction of stone blocks that was positioned along the local Roman road that ran SE-ward. The same author proposes that the extraction site was owned by a family of stonecutters that carved the Roman stele (known as "Stari dedec") into the massive limestone block that stands at the entrance to the same valley; figs. 2, 3a). If this hypothesis is true, the extraction of blocks was likely facilitated by the above-mentioned sub-vertical fractures. Interestingly, it looks is if the road-cut of the potential Roman road (located in the lower right corner of the fig. 2) follows the same fracture zone. On the walls of the road-cut we noticed indices of dextral strike slip movement.

Although the described features point to rock-cutting activities during the Roman period in the Staje area, more precise archaeological research is needed, because rock-extraction and road-construction could easily be of later origin. For example, lime production is reported from the Staje area (Dozet, 2014).

Description of the Staje section

With the Staje section 39.4 stratigraphic meters of Lower Jurassic carbonates were logged. The tentative productive part (main escarpment) of the presumed Roman quarry starts at 4.3 m and ends at 11 m of the section (fig. 3b). It is possible that there is a minor fault at the base of the escarpment (fig. 4).

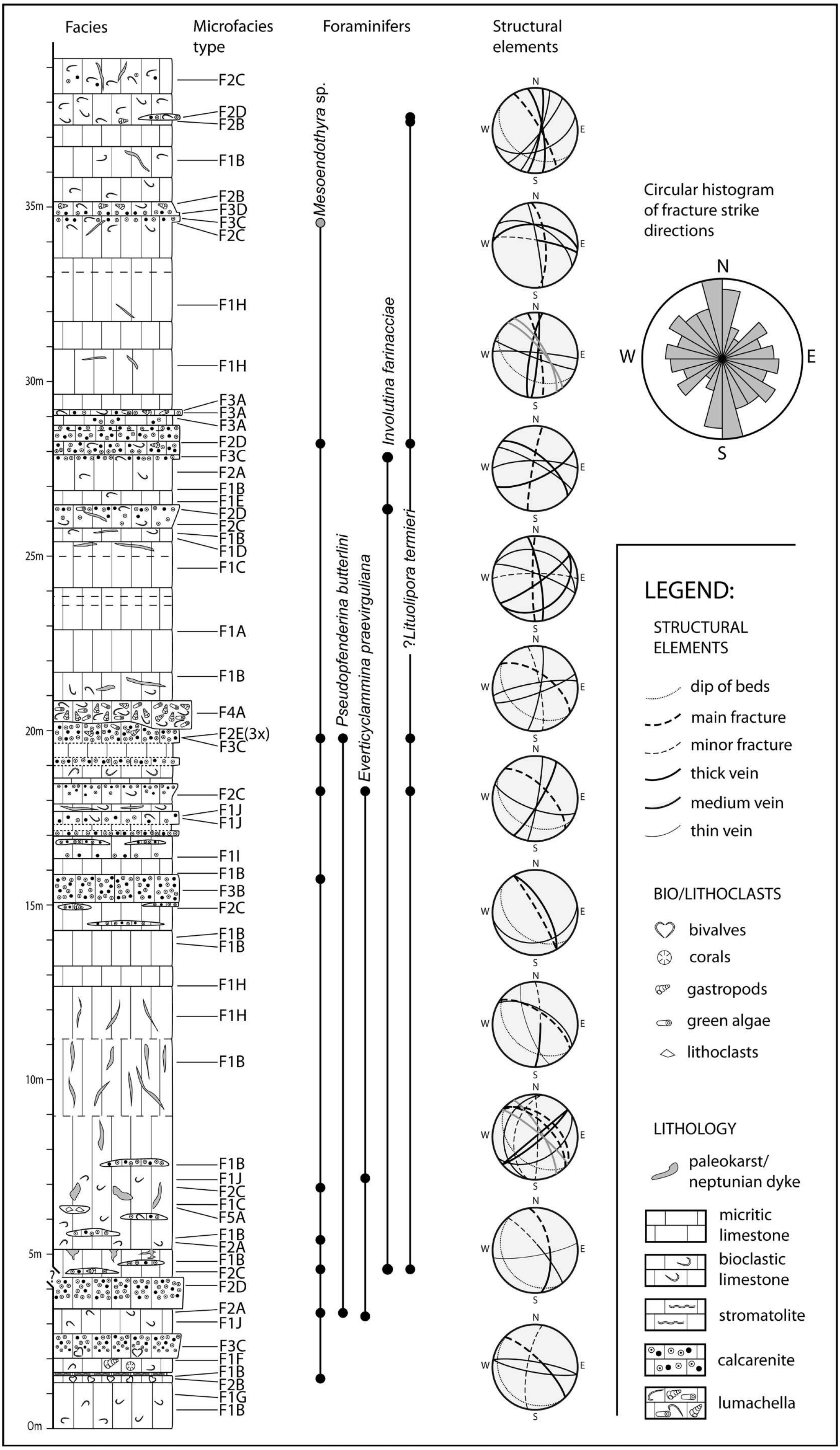

Fig. 4. Staje section with position of microfacies types, time-diagnostic foraminifers and nature of deformation at particular interval of the section (presented as spherical projection; equal-area projection, lower hemisphere and compiled in circular histogram of fracture strike directions).

The predominant facies are grey to dark grey micritic and bioclastic limestones, representing most of the thick beds, including the massive wall of the potential Roman quarry. Micritic limestone (F1) is characterized by small fenestrae. Also present are large dissolution cavities filled with cement and/or reddish, rarely greenish sediment (fig. 3c). Bioclastic limestone (F2) locally contains large (cm-sized) bivalves and subordinate gastropods. A single solitary coral was also spotted. The matrix between large fossils is micritic limestone, locally calcarenite. Besides fragments of mollusks, some beds are rich in other bioclasts: for example, the bed at the 20th m of the section also contains abundant dasycladacean algae. The third facies is grey, thin- to medium-bedded calcarenite (F3) that also occurs in thin lenses within the micritic and bioclastic facies. It is present at the base of the section (from the 2nd to 4th m), becomes more common in the middle part (15th to 20th m) and also occurs in the upper part of the section (28th to 29th and at 35th m).

The next facies type could be described as lumachella (F4) as bioclasts (gastropods, bivalves and dasycladacean algae) are accumulated in a bed at the 20.5th m of the section that shows scour-like depressions at the base (fig. 3d). A thin lens (channel) of limestone microbreccia (F5) was spotted at the 6.3th m of the section within micritic limestone. At the base of the section a thin stromatolite bed (F6) is present (no thin section was made from this facies). Neptunian dykes are present in the form of fractures filled by calcite and sediment.

Microfacies of the Staje section

The greatest diversity of microfacies was found within micritic limestone, as it is also the most common facies. *Mudstone* (F1A) appears in a single thin-section. The most common is *fenestral mudstone/wackestone* (F1B). Apart from sporadic ostracods, it is very poor in fossils. Dissolution voids are usually of two generations. Earlier, smaller (mm-sized) and usually geopetally filled birds-eyes fenestrae. These are followed by larger dissolution cavities, filled with sediment and/or cement (Figs. 5a-c). The following microfacies types are generally similar to the previous one (F1B), but have specific characteristics. In *fenestral laminated mudstone* (F1C) dense, curly laminae are visible. *Fenestral mudstone with clusters of small circular grains* (F1D) shows intense dissolution and microsparite fields that contain small circular microsparite grains (Figs. 5d. e). *Disintegrated laminated mudstone* (F1E) is composed of intraclasts that originated from disintegration of laminated mudstone (fig. 5f).

The following five microfacies are macroscopically defined as micritic limestone, but show transitional characteristics. Fenestral mudstone with large gastropods (F1F) is mudstone that contains rare larger gastropods and already represents transition to bioclastic limestone (fig. 6a). *Fenestral pelletal packstone* (F1G) and *Parallel and low-angle cross-laminated pelletal pack/grainstone* (F1H) are packstones composed of small pellets. The first is non-laminated with two generations of dissolution voids (equal to F1B) (fig. 6b). The second is laminated packstone with fenestrae present only occasionally in the form of small, lamination-parallel birds-eyes (Figs. 6c, d). *Bioturbated intraclastic/pelletal wackestone* (F1I) is wackestone that contains sand-size grains of the same type as encountered in calcarenite (fig. 6e). *Fenestral wackestone with coated grains (oncoids)* (F1J) also shows transitional characteristics to the bioclastic limestone. It generally corresponds to previously described microfacies, but additionally contains large, coated bioclasts (fig. 6f), sometimes in the form of well-developed oncoids.

Bioclastic limestone occurs in form of five microfacies. The first is *Bioclastic wackestone with or without large mollusks* (F2A). Large fossils, when present, are cm-sized (fig. 7a). In some thin sections, the density of large fossils is high and the microfacies is better described as *molluskan floatstone* (F2B) (figs. 7b, c). Two other microfacies types are found within this group. They both have large bioclasts (mostly mollusks), but the matrix between them is grain-supported (figs. 7d, e), in the form of either (partly washed) packstone (*intraclastic, ooidal, pelletal partly-washed packstone with large bivalves and intraclasts* – F2C) or grainstone (*intraclastic, ooidal, pelletal grainstone with large mollusks and intraclasts* – F2D). The last microfacies, *dasycladacean & molluskan pack/floatstone* (F2E) is transitional to ooidal calcarenite, because it contains ooidal, partly-washed packstone as a matrix and large mollusks and dasycladacean algae (fig. 7f).

Calcarenite can be divided into two subgroups according to its composition. In the first, aggregate grains prevail among the constituents (figs. 8a-c). These microfacies types are either poorly sorted, partly-washed packstone that locally contain large bioclasts (*partly washed packstone with aggregate grains* - F3B) or well sorted grainstone (*grainstone with aggregate grains* - F3A). The second subgroup is dominated by ooids (fig.

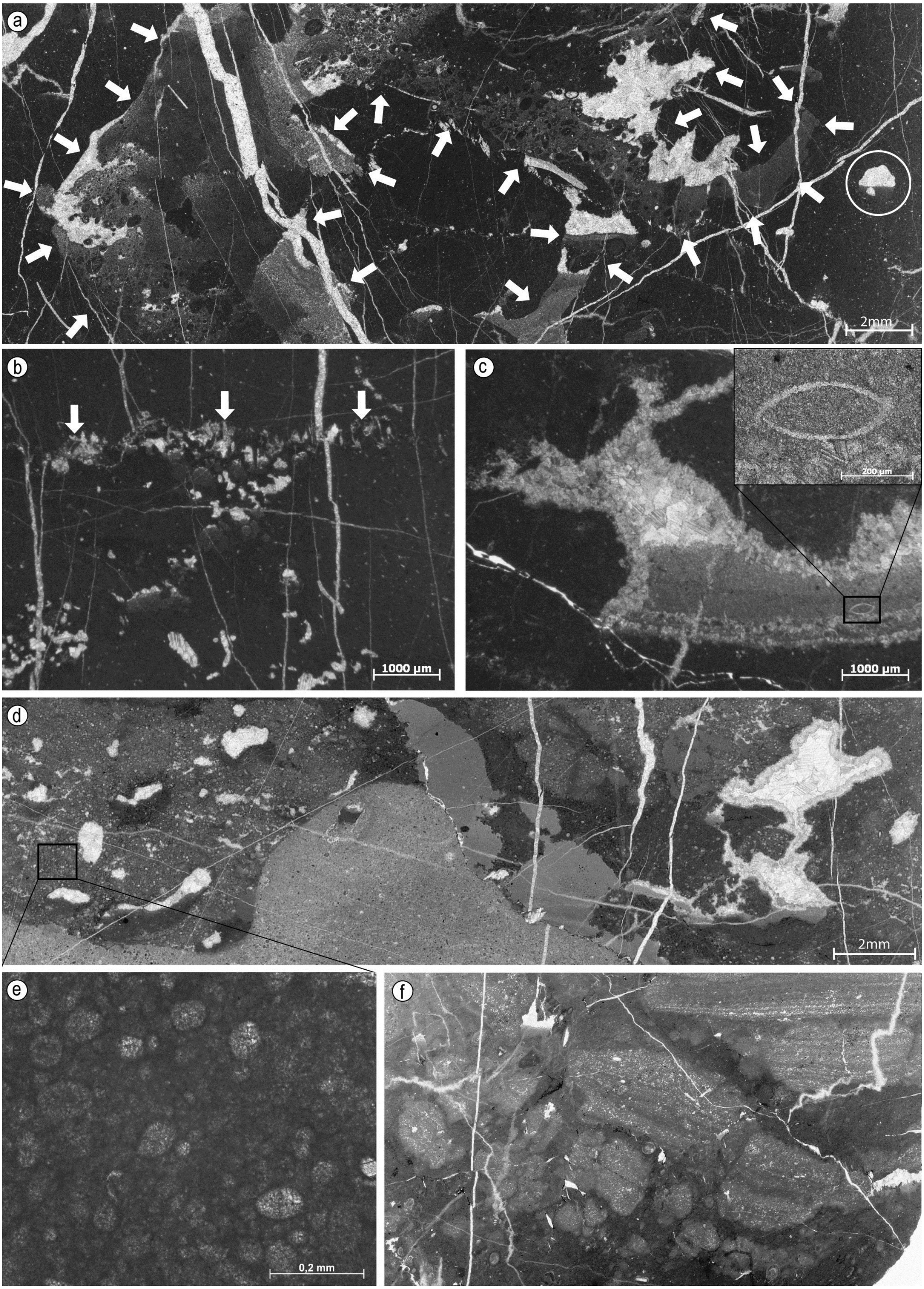

Fig. 5. Microfacies of micritic limestone.

8d), mainly in the form of *ooidal grainstone and subordinate packstone* (F3C). One thin section is *ooidal packstone with fenestrae* (F3D) that shows an intense dissolution of matrix between ooids (fig. 8e).

The last two (micro) facies types appear as coarse-grained accumulations at only two levels (figs. 8f, g). Lumachella is described as *dasycladacean & molluskan rudstone* (F4A) because it consists almost exclusively of large (cm-sized) gastropods, bivalves and dasycladacean algae (fig. 8f). Limestone microbreccia, named *lithoclastic floatstone* (F4A), is composed of diverse, angular lithoclasts and comes from a thin lens (?channel) within micritic limestone (fig. 8g). For a detailed description of microfacies see Table 1.

Biostratigraphy of the Staje section

The foraminiferal assemblage within the investigated succession (fig. 9) is characterized by *Pseudopfenderina butterlini* (Brun), *Mesoendothyra* sp., *Everticyclammina praevirguliana* Fugagnoli and ?*Lituolipora termieri* (Hottinger). The uncertainties in the structure of the wall and the type of aperture prevent us from reliably determining the latter species. The stratigraphic range of *P. butterlini* is from late Sinemurian to Pliensbachian (BouDagher-Fadel & Bosence, 2007; Velić, 2007). Due to the absence of lithiotid bivalves and *Orbitopsella* in the section, we suggest Sinemurian age for the studied succession. *Mesoendothyra* sp. likewise makes its first appearance in Sinemurian (Velić, 2007), whereas *E. praevirguliana* possibly appears already in the latest Hettangian (Velić, 2007) or during the Sinemurian (BouDagher-Fadel & Bosence, 2007). Other associated foraminiferal species, all with long stratigraphic ranges or not considered to be reliable biostratigraphic fossils, are *Duotaxis metula* Kristan, *Siphovalvulina* ex gr. *gibraltarensis* BouDagher-Fadel et al., *Siphovalvulina colomi* BouDagher-Fadel et al. vel *Siphovalvulina variabilis* Septfontaine, *Earlandia dunningtoni* (Elliot), *Involutina farinacciae* Brönnimann & Koehn-Zaninetti, ?*Trocholina umbo* (Frentzen), *Ammobaculites* sp., *Reophax* sp., Textulariidae, undetermined miliolid and lagenid foraminifers.

Neptunian dykes and other structural elements

Neptunian dykes occur in the form of thick extensional fractures with a NW-SE strike and dipping generally perpendicular to the bedding of the host-rock, but other directions are also present. Infilling of fractures vary from: A) completely sediment-filled fractures, B) sediment fill that follows the first generation of cements (usually with crystal growth perpendicular to fracture margin), C) geopetally filled fractures (often after the first generation of cement), and D) fractures filled with calcite and fragments of host-rock. The thick, calcite-filled veins probably belong to the same extensional event. The combinations and vertical alternation of the described subtypes (including thick veins) can be visible in the same thin-section (fig. 10a).

Sediment of neptunian dykes varies from calcisiltite to medium-grained calcarenite; occasionally it even alternates irregularly or in laminae within the same dyke (figs. 10b-d). Most information comes from the dyke at 6.4 m of the section that is filled with coarse calcarenite (Fig. 10d). It is well-sorted medium-grained packstone composed predominantly of bioclasts, intraclasts, pellets and subordinate small, superficial ooids. Among the bioclasts echinoderm fragments prevail. Others are foraminifers, *Tubiphytes*-like grains, fragmented bivalves and fragments of dasycladacean algae. Part of the sparitic grains could also originate from the disintegration of early cements.

Fig. 5. Microfacies of micritic limestone

a) Fenestral wackestone with large void filled by several generations of cement and sediment. Arrows indicate margins between large cavity and host rock. Circle (right side of micrograph) envelops birds-eyes void filled geopetally with ostracod-bearing calcisiltite and drusy-mosaic calcite (mf-type F1B, sample 14.1).

b) Field of small fenestrae (some geopetally infilled) that are divided by a network of thin micritic walls (mf-type F1B, sample 0.5).

c) Geopetal infill of stromatactis with two generations of cement and intermediate sediment infill with calcisiltite. In boxed area an ostracod from calcisiltite is enlarged (mf-type F1B, sample 21.6).

d) Fenestral mudstone with clusters of small circular grains (enlarged in fig. 1e). Early fenestrae tend to form in micrite between these clusters. Later generations of dissolution voids (filled with calcisiltite) are larger and do not follow the preceding texture (mf-type F1D, sample 25.5).

e) Enlarged cluster with small oval microsparitic grains that may be produced through early diagenetic bacterial-induced cementation (mf-type F1D, sample 25.5).

f) Disintegrated laminated mudstone. Downwards, intraclasts tend to decrease in size and oval, mm-sized grains (?pisoids) start to occur between them (mf-type F1E, sample 26.55).

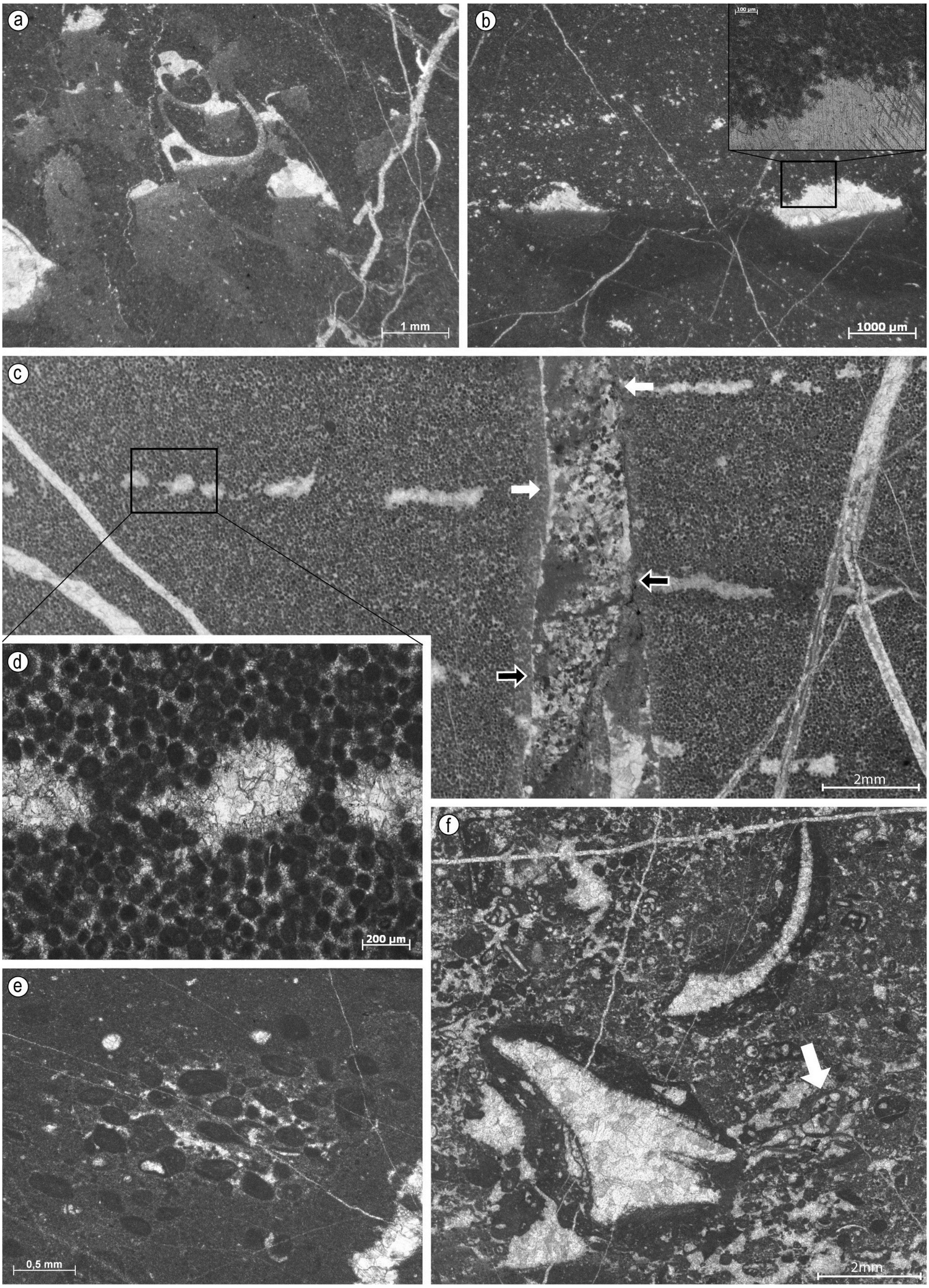

Fig. 6. Transitional microfacies from micritic to other microfacies.

a) Mudstone with gastropod shell involved in formation of fenestrae (mf-type F1F, sample 1.9).

b) Pelletal packstone with fenestrae filled by dense micrite, dissolved again and geopetally refilled. The enlarged box shows that the host-rock is composed of densely packed tiny pellets (mf-type F1G, sample 1.0).

c) Pelletal packstone with fenestrae occurring mostly in distinct laminae (enlarged in Fig. 6d). Fracture is filled with latest Jurassic sediment (neptunian dyke); arrows indicate minor displacement (mf-type F1H, sample 32.2).

d) Birds-eyes laminae within pelletal packstone (enlargement of boxed area from Fig. 6c) (mf-type F1H, sample 32.2).

e) Intraclasts and pellets concentrated in burrow inside wackestone that contains equal grains (mf-type F1I, sample 16.3).

f) Coated bioclasts within fenestral wackestone; arrow indicates Thaumatoporella sp. (mf-type F1J, sample 3.1).

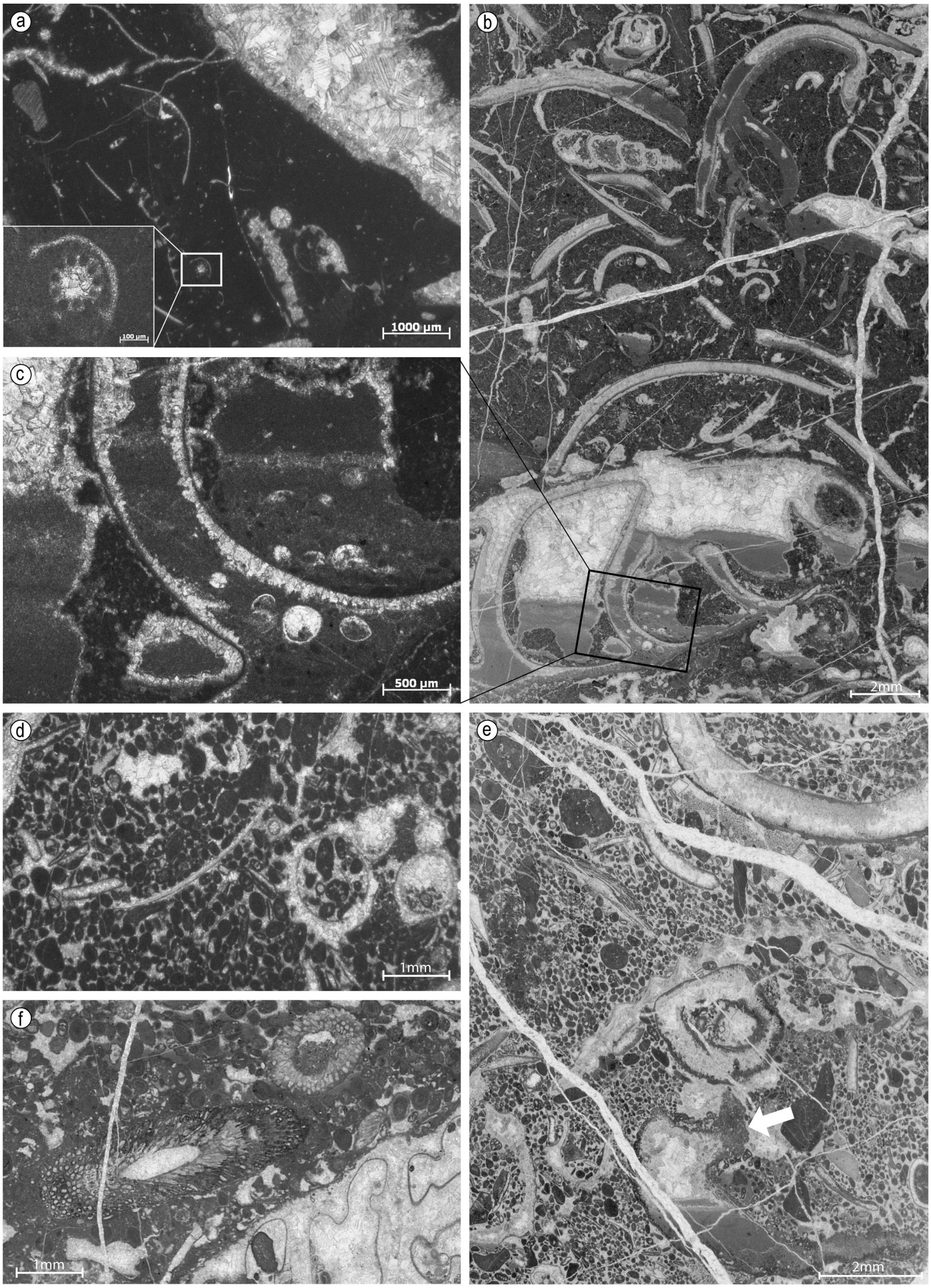

Fig. 7. Microfacies of bioclastic limestone.

a) Bioclastic wackestone with large recrystallized bivalve. Small circular grain (enlarged in boxed area) could be gyrogonites (mf-type F2A, sample 27.4).

b) Gastropods and bivalves as main cm-sized grains in floatstone (boxed area enlarged in Fig. 7c) (mf-type F2B, sample 35.1).

c) Complex pattern of poly-generation dissolution and subsequent infilling of bioclastic floatstone as a result of repeatable subaerial exposure (enlargement of boxed area from Fig. 7b) (mf-type F2B, sample 35.1).

d) Gastropod and bivalve within generally finer partly-washed packstone (mf-type F2C, sample 18.2).

e) Large fossils (bivalves, brachiopod, dasycladacean algae) and intraclasts inside intra/bioclastic and ooidal grainstone. Arrow indicates microbial crusts on completely dissolved and geopetally infilled grain, probably bivalve in origin (mf-type F2D, sample 26.35).

f) Dasycladacean algae and large gastropod inside ooidal and intraclastic partly-washed packstone (mf-type F2E, sample 19.8).

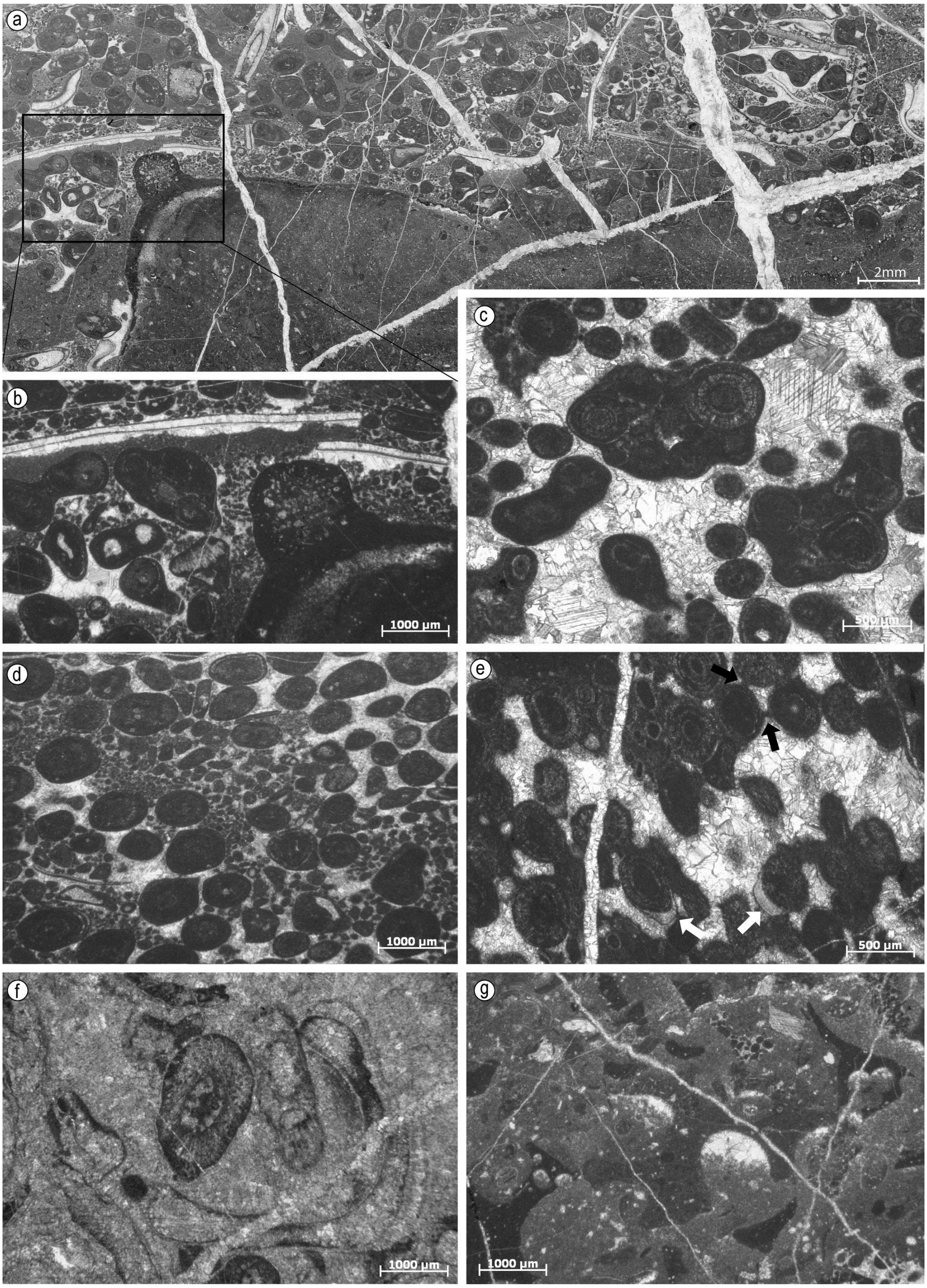

Fig. 8. Microfacies of calcarenite, lumachella and litoclastic microbreccia.

a) Hardground with irregular surface ending with encrusting organisms (boxed are enlarged in Fig. 8b) and overlain by partly-washed packstone with aggregate grains and large bioclasts, mainly bivalves and dasycladacean algae (mf-type F3A, sample 28.95).

b) Encrusting organism at the surface of the hardground and structure below bivalve shells (enlarged from boxed area in fig. 8a) (mf-type F3A, sample 28.95).

c) Grainstone composed of aggregate grains and ooids (mf-type F3B, sample 15.4).

d) Laminae of pelletal packstone within ooidal grainstone (mf-type F3C, sample 2.3).

e) Ooidal packstone with dissolution voids often selective to matrix. Cements are fibrous-rim, drusy-mosaic and possibly stalactitic (white arrows) and micritic meniscus (black arrows) cements. The latter could also represent the remains of an undissolved matrix that remained close to contacts of dissolution-resistant ooids (mf-type F3D, sample 34.8).

e) Recrystallized dasycladacean algae and mollusks inside rudstone (mf-type F4A, sample 20.5).

f) Diverse lithoclasts that form a floatstone matrix. Note that the margins of lithoclasts are highly irregular, which points to very short transport. Some also show burrows at margins (mf-type F5A, sample 6.3).

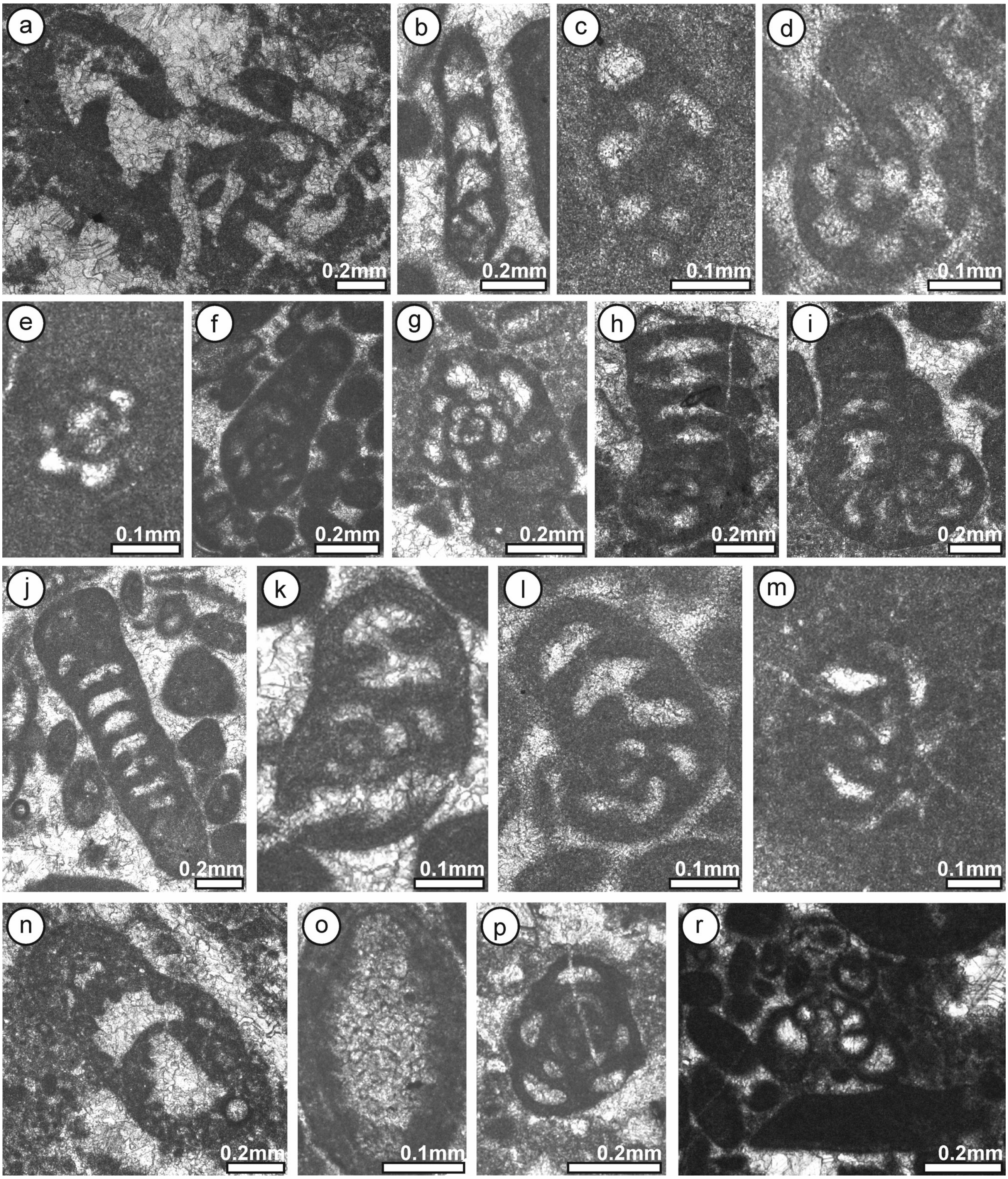

Fig. 9. Foraminifers from the logged Staje succession.

a-b: *Everticyclammina praevirguliana* Fugagnoli. Thin sections 4.1 and 18.2, respectively.

c: *Pseudopfenderina butterlini* (Brun). Thin section 3.3.

d-g: *Mesoendothyra* sp. 4: Thin section 18.2. 5: Thin section 5.3. 6: Thin section 4.5. 7: Thin section 34.55.

h-m: ?*Lituolipora termieri* (Hottinger). 8-10: Thin section 37.55. 11: Thin section 28.25. 12: Thin section 18.2. 13: Thin section 5.3.

n: Undetermined Lituolida. Note canaliculate wall structure. Thin section 7.1.

o: *Involutina farinacciae* Brönnimann & Koehn-Zaninetti. Thin section 15.9.

p: ?*Quinqueloculina* sp. Thin section 5.4. Infill of neptunian dyke.

r: *Siphovalvulina ex gr. gibraltarensis* BouDagher-Fadel, Rose, Bosence & Lord. Thin section 25.9.

Table 1. Microfacies types of the Staje section. Standard Microfacies types (SMF) are summarized after Flügel (2004). Please note that fenestrae are considered as generally synsedimentary and are described within the composition (including infill sediment and cements) of the particular microfacies type.

Facies	Microfacies	Description
F1 – Micritic limestone	F1A – Mudstone Sample 22.8	**Composition:** Micrite strongly predominates. Very rare are small, oval sparitic grains (bioclasts). **Diagenesis:** Contains dense network of thin calcite veins. **SMF / environment:** SMF23 / Supra-intertidal, restricted lagoon.
	F1B - Fenestral mud/wackestone Samples 0.5, 1.0, 1.5, 4.8, 5.4, 7.6, 10.5, 13.9, 14.1, 15.8, 21.6, 25.7, 26.85, 36.3,	**Composition:** Micrite contains rare pellets and small bioclasts (fig. 5a): predominantly ostracods, very rare small bivalves and gastropods. Fenestrae are small (mm-sized) and irregular, rarely of stromatactis type or oval shaped (fig. 5c). Infillings show geopetal structures: micrite/calcisiltite (laminated, can contain ostracods) is at the bottom, while the top is filled with mosaic calcite. Some fenestrae (of stromatactis type) contain isopachous fibrous rim cements that can post- or pre-date calcisiltite fill. Some small-scale fenestrae in sample 0.5 are grouped in larger fields and divided by very thin, undulated micrite films, thus forming an irregular, geopetally filled mesh (fig. 5b). Large (cm-sized) dissolution voids locally post-date fenestrae. They are irregular, mostly filled by isopachous fibrous or drusy-mosaic cements. Some are filled with mudstone with ostracods. Large void in sample 14.1 shows complex multi-generation filling with peloidal/intraclastic/ooidal packstone that either grades or sharply passes to mudstone. Older fillings exhibit partial dissolution (fig. 5a). **Diagenesis:** Locally, micrite is recrystallized to microsparite. Present are stylolites and dense network of thin, occasionally thicker calcite veins. Some fractures in samples 4.8 and 5.4 are filled by younger sediment (neptunian dykes). Sample 4.8 shows dispersed dolomite crystals close to and inside of neptunian dyke. **SMF / environment:** SMF21 / Supra-intertidal, restricted lagoon; repeatable periods of post-depositional subaerial exposure.
	F1C - Fenestral laminated mudstone Samples 6.4, 24.7	**Composition:** Irregular laminae of dense, aphanitic micrite with rare ostracods alternate with microsparite with birds-eyes fenestrae of various sizes. Aphanitic micrite may laterally pass into pelletal micrite. Fenestrae are filled by mosaic calcite cement. **Diagenesis:** Thin calcite veins run in various directions. Sample 24.7 has thicker calcite veins oriented sub parallel to laminae. Laminated mudstone in sample 6.4 shows almost complete dolomitization: dolomite is slightly reddish; dense micritic laminae remain partly preserved in irregular fields. **SMF / environment:** ?SMF 19 / Supra-intertidal, restricted lagoon.
	F1D - Fenestral mudstone with clusters of small circular grains Sample 25.5	**Composition:** Micrite contains highly irregular – cauliflower-like bodies of microsparite with abundant small circular grains (sometimes sparite, sometimes with sparitic rim and micritic core) (figs. 5d, e). These bodies could originate during early diagenetic (?bacterial-induced) cementation. Micrite shows compaction along the margins with microsparite. It can contain very rare ostracods. Fenestrae can be birds-eyes or very irregular and tend to appear selectively in micrite between the microsparite bodies. Larger have complete or geopetal filling with calcisiltite. Upper parts of partly filled fenestrae often show two generations of cementation. First-formed is the isopachous rim cement (can be followed by second generation of calcisiltite fill). The second cement is drusy-mosaic calcite. Large (cm-sized) dissolution voids (younger than fenestrae) are irregular, filled by mud/wackestone with very small pellets. Infill sediment can contain last generation of small birds-eyes filled with drusy-mosaic calcite. **Diagenesis:** Pyrite occurs along the stylolites or in form of rare framboidal pyrite within the sediment **SMF / environment:** SMF21 / Supra-intertidal, restricted lagoon; repeating periods of subaerial exposure.
	F1E - Disintegrated laminated mudstone Sample 26.55	**Composition:** Large (cm-sized) intraclasts of dense laminated mudstone that show partly fitted fabrics are sunk into underlying micrite (fig. 5f). Downwards, intraclasts are progressively smaller and more rounded. Small, geopetally filled birds-eyes fenestrae occur inside and between intraclasts. The micrite in the lower part of the thin-section contains rare coated grains (?pisoids) and a foraminifer. Few coated grains occur also in matrix between the intraclasts. **Diagenesis:** Thin calcite veins run in various directions. Pyrite occurs along stylolites and small dissolution seams within micrite. **SMF / environment:** ?SMF24 / Restricted lagoon.
	F1F - Fenestral mudstone with large gastropods Sample 1.9	**Composition:** Very rare small bioclasts (recognizable are bivalve fragments), and up to a few mm large gastropods, which can have geopetal infilling (fig. 6a). Two kinds of dissolution voids are present: -smaller fenestrae: these usually contain geopetal infill with micrite/calcisiltite and drusy-mosaic calcite. Some have thin calcite rim that formed prior to sediment infill. Dissolution occasionally includes the walls of gastropod shells and also the primary micrite infill of shell-cavities. -large (cm-sized) irregular dissolution voids infilled with large micrite intraclasts (originating from collapse of the void roof) and calcisiltite, occasionally with pellets. **Diagenesis:** Network of thin calcite veins that run in various directions. Other features are stylolites and rare framboidal pyrite. **SMF / environment:** Between SMF21 and SMF12 / Lagoon (restricted); repeating periods of subaerial exposure.
	F1G - Fenestral pelletal packstone Sample 1.0	**Composition:** Pellets are small and densely packed. Small bioclastic fragments are present but rare. Three types of dissolution voids can be recognized (fig. 6b): -small fenestrae filled with drusy-mosaic calcite, -large cm-sized irregular dissolution voids filled with micrite containing rare ostracods and small bioclastic fragments, -small fenestrae occurring solely inside or at upper margins of micrite infills of large voids; these fenestrae show geopetal infill with calcisiltite and drusy-mosaic calcite. **Diagenesis:** Network of thin calcite veins that run in various directions. Stylolites occur. **SMF / environment:** Between SMF16-NONLAMINATED and SMF21 / Restricted lagoon; repeating periods of subaerial exposure.

	F1H - Parallel and low-angle cross laminated pelletal pack/grainstone Samples 11.8, 12.7, 30.45, 32.2	**Composition:** Pellets predominate. Subordinate are small bioclastic fragments (mostly unrecognizable, some fragmented shells, echinoderms and foraminifers). Some laminae have grainstone texture. They contain larger grains, including superficial ooids and cortoids. Sample 32.2 contains elongated fenestrae (birds-eyes) that replace certain bedding-parallel laminae or are (more rarely) curved. Infill is drusy-mosaic calcite (figs. 6c, d). **Diagenesis:** Network of thin calcite veins that run in various directions. Stylolites are rare. Samples 11.8 and 12.7 have large coarse-crystalline calcite veins. Sample 32.2 has large fractures, partly filled by coarse-crystalline calcite and subsequent sediment, which is alternating with levels of calcisiltite and bio/intraclastic fine-grained packstone. **SMF / environment:** SMF16-LAMINATED; sample 32.2 has characteristics also of SMF 21 / Restricted lagoon.
	F1I - Bioturbated intraclastic/ pelletal wackestone Sample 16.3	**Composition:** The amount of grains is variable, mostly due to bioturbation (Fig. 6e) and also bedding-parallel lamination. Grains are represented by intraclasts, peloids and pellets, rare micritized ooids, and very rare bioclasts (echinoderm plates, bivalve shells and small gastropods). Rare fenestrae occur in form of small irregular voids or larger stromatactis; both are filled with drusy-mosaic cement. **Diagenesis:** Network of thin calcite veins that run in various directions. Sample contains large fractures that are partly filled by coarse-crystalline calcite and partly by calcisiltite (?neptunian dyke) **SMF / environment:** ?SMF24 / Structural inversion: low energy (lagoonal) mud with grains from environment of higher energy (intraclasts, ooids).
	F1J - Fenestral wackestone with coated grains (oncoids) Samples 3.1, 7.1, 17.5, 17.6	**Composition:** Main constituents are foraminifer, intraclasts and aggregate grains (simple lumps composed of few, up to 0.5 mm large ooids and intraclasts). Quantity of individual constituents varies significantly between the thin-sections (lumps are dominated in sample 17.5, foraminifers in samples 3.1 and 7.1). Other grains are ooids (sample 17.5) and diverse bioclasts: bivalves, ostracods, dasycladacean algae (sample 3.1), oval *Tubiphytes*-like grains (sample 3.1, 7.1), *Thaumatoporella* sp. (sample 3.1, 7.1, 17.6), echinoderm plates and spines. Sample 17.6 has cm-sized bivalve, that was dissolved, geopetally filled with calcisiltite with peloids and large-crystalline drusy-mosaic calcite. Matrix occasionally reveals a composition of small, densely packed pellets. Coated grains have bioclastic core (Fig. 6f; bivalves, dasycladaceas). Some are well developed (rounded) oncoids, others have thin coatings and mimic the original shape of a core. Coatings are mostly by filamentous mats (sometimes with clearly visible filaments), but encrusting foraminifers also occur. Fenestrae are present and are geopetally filled with calcisiltite/micrite and drusy-mosaic calcite. Samples 7.1 and 17.5 show bioturbation. **Diagenesis:** Network of thin calcite veins that run in various directions. Stylolites occur. **SMF / environment:** SMF 8-9 and SMF 22 / Open-marine lagoon close to more restricted environment; subaerial exposure.
F2 – Bioclastic limestone	F2A – Bioclastic wackestone with or without large mollusks Samples 3.3, 5.3, 27.4	**Composition:** Bioclasts are bivalves, gastropods, foraminifers, ostracods and small unrecognizable detritus. In sample 27.4 echinoderm spines are present. There are similar, but poly-crystalline oval grains with radially distributed rim of small circular cavities. They resemble gyrogonites or small dasycladacean algae (Fig. 7a), but show no central cavity. Other grains are pellets and in sample 3.3 also intraclasts. Samples 3.3 and 27.4 contain rare large bivalves and sample 27.4 also a large gastropod. Sample 3.3 has burrows filled by pelletal packstone and sparite. Fenestrae are present and are geopetally filled with calcisiltite and drusy-mosaic calcite. In sample 3.3 they occur in burrows. Large bivalves were dissolved and replaced by drusy-mosaic calcite, in case of sample 37.4 molds were first lined by thin rim-cement. **Diagenesis:** Network of thin calcite veins that run in various directions. Thick fractures are filled mostly by drusy-mosaic calcite, but in sample 27.4 the fracture (neptunian dyke) has geopetal fill with calcisiltite, showing different orientation than in fenestrae (fig. 10c). Stylolites are present and sample 27.4 has rare framboidal pyrite **SMF / environment:** SMF8 and SMF9 / Open-marine lagoon with subaerial exposure.
	F2B – Molluskan floatstone Samples 1.4, 35.1, 37.4	**Composition:** Large (cm-sized) mollusks float in bioclastic wackestone matrix (fig. 7b). Sample 1.4 contains thick-shelled bivalves. In samples 35.1 and 37.4, gastropods and medium-thick shells of bivalves predominate, but sample 37.4 contains fragmented thick-shelled bivalve with multi-layered prismatic texture. Bioclasts in matrix are small (mm-sized), frequently fragmented bivalves, gastropods, ostracods and foraminifers. Sample 35.1 contains dasycladacean algae and 37.4 crinoids. Intraclasts and subordinate micritized ooids were locally observed. All samples show intense dissolution: -most intense dissolution attacked large bioclasts, and places with largest concentration of fossils, dissolution often deviates from shells to surrounding matrix, -isolated fenestrae within the matrix are rare. Multiple generations of infill can be seen in voids: -the first generation is thin rim-cements (not observed in sample 37.4), -the second is a geopetal infill by calcisiltite (in sample 35.1 with ostracods and 37.4 with small intraclasts/pellets), -in sample 35.1, it is followed by the second generation of thin rim-cement (some parts show even more complex alternation of rim cements and sediment infills; figs. 7b, c). -large-crystalline, isopachous rim (often bladed) or drusy-mosaic cement, -matrix in sample 35.1 shows dense network of irregular thin fractures filled with calcite, which we attribute to the desiccation. **Diagenesis:** Network of thin calcite veins that run in various directions. Stylolites occur. Sample 1.4 has wide fracture partly filled with large calcite (occasionally bladed) and subsequent sediment: very-fine packstone with pellets or calcisiltite (it could either be neptunian dyke or coarser synsedimentry infill of larger dissolution void). In sample 35.1 is mm-size field of pyrite. Sample 37.4 has system of brown-coloured (?pyrite) carbonate veins. **SMF / environment:** SMF8 / Open-marine lagoon with at least one longer period of subaerial exposure.

	F2C – Intraclastic, ooidal, pelletal partly-washed packstone with large bivalves and intraclasts Samples 4.5, 6.9, 14.9, 18.2, 25.9, 34,55, 38.7	**Composition:** The commonest grains are intraclasts, ooids (mostly micritisized), and pellets. Other subordinate grains are cortoids and bioclasts: foraminifers, small and mostly fragmented bivalves, echinoderms (sample 6.9), *Tubiphytes*–like fossils, calcimicrobes (sample 4.5). Large (few-mm sized) grains float within the packstone matrix and are mostly bivalves and intraclasts. Subordinate are gastropods (Fig. 7d; samples 14.9, 18.2, 25.9) and brachiopods (samples 25.9, 34.55). Large bioclasts tend to be completely recrystallized. Intraclasts reveal primary structure of mudstone or wackestone with ostracods, fragmented bivalves, and other small biodetritus. Sample 4.5 has large intraclast of pelletal and ooidal packstone with micritic rim. Sample 6.9 is partly washed-out packstone, composed mostly of intraclasts and pellets, and contains fenestrae. **Diagenesis:** Network of thin calcite veins that run in various directions. Thick fractures are filled mostly by drusy-mosaic calcite; in sample 4.5 also calcisiltite (neptunian dyke). Some thick, calcitic veins in sample 4.5 are unusually curved. In sample 34.55, one thick vein is brown colored and contains pyrite. Stylolites were noticed and small dispersed pyrite occurs in samples 25.9 and 34.55. **SMF / environment:** ?SMF8-18, close to SMF11 / Open-marine, low- energy lagoon; subaerial exposure.
	F2D – Intraclastic, ooidal, pelletal grainstone with large mollusks and intraclasts Samples 4.1, 26.35, 28.25, 37.55	**Composition:** Bimodal grain-size (fig. 7e). Small grains are intraclasts and pellets, subordinate are ooids (often superficial and/or micritized), cortoids (mostly from bivalve fragments) and foraminifers. Rare are echinoderms and *Tubiphytes*–like fossils. In sample 4.1 aggregate grains (lumps) were also observed. Large grains are predominantly bivalves (thick to medium shelled) and gastropods, but brachiopods and dasycladacean algae are also present. Most samples (4.1, 26.35, 37.55) have also large, well rounded mudstone intraclasts, which in sample 4.1 tend to be dolomitized. Large grains tend to have endolithic margins or overgrowths of calcimicrobes (filaments are still visible) or encrusting foraminifers. Shells are recrystallized or were dissolved and filled with cement. In sample 26.35, one such fossil has geopetal infill with calcisiltite, a thin rim-cement and subsequent drusy-mosaic cement. Same grains have thin calcimicrobial overgrowth. Bellow large shells shelter pores are common. Thin micritized surface (?hardground level) was observed in sample 28.25. Sample 26.35 has few fenestrae in local very-fine grain/packstone that occurs bellow shelter structure. Fenestrae are lined with thin rim-cement and filled with drusy-mosaic cement. **Diagenesis: N**etwork of thin calcite veins that run in various directions, but thicker calcite veins also occur. Sample 26.35 has pyrite concentrated in some micritic grains (particularly in larger intraclasts). Sample 4.1 has selective dolomitisation of micritic grains, particularly the large intraclasts. Sample 37.55 has stylolites with adjacent minor dolomitisation. **SMF / environment:** ?SMF8-10 / High-energy environment (or event) within open-marine lagoon. Sample 26.35 shows subaerial exposure.
	F2E – Dasycladacean & molluskan pack/floatstone Sample 19.8 (several thin sections)	**Composition:** Large grains are dasycladacean algae, bivalves and gastropods (fig. 7f). Rare are cm-sized mud/wackestone intraclasts with pellets and small biodetritus. Matrix between large fossils is partly-washed packstone composed of ooids (mostly micritized) and pellets, subordinate are foraminifera, cortoids, intraclasts and unrecognizable biodetritus. Rare are smaller bivalves, fragmented dasycladaceas, *Tubiphytes*- like grains, echinoderm plates. Fenestrae are mm-sized and highly irregular. They are filled with thin isopachous rim cement followed by drusy-mosaic cement. The same cements are observed in mollusks, particularly the walls of gastropod shells. **Diagenesis:** Network of thin calcite veins that run in various directions, but one direction prevails (one of these veins is thicker). One thin-section exhibits highly irregular "vein" that could be larger, elongated dissolution void. Pyrite rarely occurs in dispersed framboids or small clusters. **SMF / environment:** SMF18 / Open-marine, close to ooidal shoals; subaerial exposure.
F3 - Calcarenite	F3A – Partly washed packstone with aggregate grains Samples 28.95, 29.1, 29.2	**Composition:** The main components are aggregate grains (fig. 8a). In sample 28.95, their average size is from 1.46 to 1.69 mm, with largest being a few millimetres long. They are lumps composed of several medium-sized grains, mostly ooids, but pellets, intraclasts and bioclasts also occur. Other rare, sand-size grains are ooids (mostly micritized), intraclasts and bioclasts (often with microbial crusts): bivalves, dasycladacean algae (fragments of large specimens and small whole specimens), rare crinoids, gastropods and small foraminifers. Tiny pellets occur in matrix. Large fossils occur in samples 28.95 and 29.2; these are bivalves, dasycladacean algae and rarer gastropods. Bivalves often form shelter texture. They have endolithic margins and sometimes also thin microbial overgrowths. In sample 28.95, below the herein described microfacies there is a laterally discontinuous hardground (Fig. 8a). The hardground formed on microfacies corresponding to sample 16.3 (bioturbated intra/pel wackestone). Towards the margins (vertical and lateral) it becomes micritic, with visible irregular laminae (?microbial mats). At the hardground edge there is an encrusting fossil (fig. 8b). Sample 29.2 has fenestrae with shapes adjusting to the margins of larger grains (dissolved is matrix with pellets). These voids together with shelter textures and fossil cavities are infilled geopetally by calcisiltite, radiaxial fibrous and subsequent drusy-mosaic cement. **Diagenesis:** Network of thin calcite veins that run in various directions, but thicker calcite veins also occur. Stylolites and dispersed framboidal pyrite (mostly in micritic grains and matrix) occur. Cements in grainstone parts are thin fibrous rim-cements (differ from those filling the larger voids) and drusy-mosaic calcite. **SMF / environment:** SMF 17 / Open marine lagoon established after the cessation of sedimentation and formation of agitated sea-floor (hardgrond). Sample 29.2 shows subaerial exposure.
	F3B – Grainstone with aggregate grains Sample 15.4	**Composition:** The main components are aggregate grains, ooids and pellets (fig. 8c). Average size of aggregate grains is 1.55 mm; these are lumps composed of numerous fine-to medium-grained ooids (radial and tangential) and pellets. Average size of ooids is 0.37 mm; they have five laminae; the nucleus:cortex ratio is 42:58. Other grains are bioclasts (sometimes with microbial crusts): bivalves, dasycladacean algae, cortoids and rare echinoderms and foraminifers. **Diagenesis: C**ements are thin fibrous rim-cement and subsequent drusy-mosaic calcite cement. Network of thin calcite veins that run in various directions, but thicker calcite veins also occur. **SMF / environment:** SMF 17 / High-energy environment within open marine lagoon (close to sandy shoals).

	F3C – Ooidal grainstone, subordinate packstone Samples 2.3, 19,8sp1, 27.85, 34.7	**Composition:** The main components are ooids and pellets. Pellets are small, showing bimodal size distribution and concentrated in generally thinner laminae (fig. 8d). Type and size of ooids varies from 0.37 to 0.79 mm. They have between four and six laminae, and the nucleus:cortex ratio around 44:56. They are predominantly tangential and micritized, in sample 34.7 radial ooids also occur. Other grains are bioclasts, mainly foraminifers, but fragmented bivalves, echinoderms and dasycladacean algae also occur. Sporadic are *Tubyphites*- like grains, small gastropods and cortoids, aggregate grains, intraclasts and gastropods. **Diagenesis:** Cements are thin fibrous rim-cement and subsequent drusy-mosaic cement. Sample 2.3 contains very sporadic dolomite rhomboeders in micritized ooids. Network of thin calcite veins that run in various directions. Sample 34.7 has also network of thick calcite veins. Stylolites and dispersed framboidal pyrite are rare. **SMF / environment:** SMF15 / Sandy shoals, close to the open marine lagoon.
	F3D – Ooidal packstone with fenestae Sample 34.8	**Composition:** The main components are mostly radial ooids, but tangential and small superficial ooids also occur (fig. 8e). They have average size of 0.48 mm and have six laminae. The ratio nucleus:cortex is 41:59. Other grains are pellets, rare small foraminifers. It contains also rare large bioclasts: bivalves, gastropod, mm-sized dasycladacean algae and partly recrystallized calcimicrobes. Fenestrae are of millimeter size. Ooids show some dissolution at their margins. Fenestrae and intergranular spaces are filled with thin rim cement and drusy-mosaic calcite cement. Meniscus cement occurs as pendant micrite (it could also be matrix which escaped dissolution). Microstalactitic spar cement also occurs (because orientations are in various directions, some of these cements could also be meniscus bridging cement). **Diagenesis:** Network of thin calcite veins that run in various directions. Some veins are a bit thicker, one of these shows partial infill with calcisiltite (neptunian dyke). Pyrite occurs in up to 1 mm large fields or as dispersed framboids. **SMF / environment:** ?SMF15 / Structural inversion: grains from high-energy environment (ooidal shoals) resedimented into quiet environment (lagoon); subaerial exposure.
F4 - Lumachella	F4A – Dasycladacean & molluskan rudstone Sample 20.5	**Composition:** Grains are almost exclusively cm-sized bivalves and gastopods, and mm-sized dasycladacean algae (fig. 8f). Cm-sized wackestone intraclast with fragmented bivalves and echinoderms was detected (these grains resemble those from 19.8). Bioclasts are strongly recrystallized, some have thin microbial crusts. Mollusks were probably dissolved and filled with cements. Some central cavities (medulla) of dasycladan algae contain pellets and small ooids or intraclasts. Rare small grains are ooids and intraclasts. **Diagenesis:** Intergranular pores are filled with radiaxial rim-cements followed by drusy-mosaic cements. Large dissolution void is irregular and filled with drusy-mosaic cement. Calcite veins are rare and thin. **SMF / environment:** SMF14 / Lag-deposit within or close to open marine lagoon; subaerial exposure
F5 - Limestone microbreccia	F5A – Litoclastic floatstone Sample 6.3	**Composition:** Mm- to cm-sized litoclasts within wackestone matrix with pellets and bioclasts (fig. 8g): small ostracods, echinoderms, small bivalves, oval sparitic grains (probably bioclasts). Lithoclasts are angular (some even show borings) and diverse: A) mud/wackestone, sometimes with visible pellets, small unrecognisable biodetritus, and undetermined oval sparitic grains; some are small, angular and elongated (could be mud chips), B) pelletal grain/packstone, and C) ooidal grainstone with medium-grained tangential and less frequent radial ooids, rare pellets, intraclasts, and aggregate grains. **Diagenesis:** Some mudstone lithoclasts show dispersed dolomitic rhomboeders. Network of thin calcite veins that run in various directions. **SMF / environment:** SMF 24 / Storm deposit within tidal flat or redeposited into restricted lagoon.

In the sample at 5.3 m of the section, the angle between the primary geopetal orientation and those of the neptunian dykes can reach up to 69° (fig. 10c), and in the sample from 1.4 m of the section a difference of 33° was measured (fig. 10b). From the laminations in the sample at 32.2 m of the section, the maximum difference in angle is 57°.

The neptunian dykes from the sample at 4.8 m of the section show complex evolution (fig. 10a). The first generation of dykes is irregular and filled with early generations of cement and subsequent very fine calcisiltite. The second generation cuts through the first filling of the dykes. It is represented by a thin cement layer, followed by very fine calcisiltite. Infill of the first two generations shows mostly dispersed dolomite crystals similar to those observed in the host-rock. It could point to an older (maybe even Lower Jurassic) opening of the dykes, but dolomitization could also be selective to the lithology (dolomite is more abundant in micrite and very fine calcisiltite). In the third phase, new fractures formed or the old fractures re-activated. This generation of dykes is filled primarily by coarse-crystalline calcite and sporadic fine calcisiltite, followed by a deposition of generally coarser sediment within the cracks. This sediment can be further divided into first-settled sediment, consisting of calcisiltite that contains fine-grained packstone laminae and shows some plastic deformation, whereas the youngest sediment is fine-grained packstone, and is in composition very similar to the sediment infill of the neptunian dyke from the sample at 6.4 m of the section.

Foraminifera ?*Quinqueloculina* sp. and dasycladacean algae *Clypeina jurassica* Favre (det. by R. Radoičić; fig. 10d) were found in the intra-bioclastic packstone filling of the neptunian dykes. The latter indicates infiltrated sediment of Upper Jurassic age (Chiocchini et al., 1994; Senowbari-Daryan et al., 1994).

Other structures are fractures and veins, but we emphasize that the fractures observed in the weathered rock largely follow the orientation of a particular vein-cluster. Most fractures and veins are oriented in an approximate N-S stike (fig. 3). Other veins run in the NW-SE direction. The most common veins are also the thickest, and could be extensional fractures originating from the latest Jurassic tectonic movements, but they lack the sediment infill. The azimuth and dip of the main wall of the potential Roman quarry is 60/75, and the rock behind the wall is fractured in the same direction. Other calcite veins are generally thinner and strike in various directions (commonly W-E and NE-SW) and cross cut the neptunian dykes. The azimuth and dip of the beds is constant, with small variations around 220/40.

Discussion

Sedimentary environment: The lower Lower Jurassic (Sinemurian) succession of the Staje section shows characteristics of the platform interior. The first of the dominating facies, micritic limestone, is characterized by fenestrae (birds-eyes). This facies deposited in a shallow subtidal environment such as a restricted lagoon with frequent subaerial exposure. A stromatolite bed, probably also laminated mudstone and limestone microbreccia, deposited in intertidal environment (tidal flats). The second dominating facies, bioclastic limestone, is of variable texture and shows a rich fossil assemblage. It was sedimented in an open-marine lagoon. The transition to a restricted lagoon is marked by fenestral wackestone that contains oncoids and pelletal pack/grainstone (laminated and fenestral subtypes). The lagoon was occasionally subjected to more agitated conditions (storms) as evidenced by grainstone with large bioclasts and particularly by a lumachella bed. A more agitated yet still lagoon environment can also be implied for the grain/packstone composed predominantly of aggregate grains, and ooidal grain/packstone as well. The latter was deposited at the transition to the ooid shoals.

Correlation: In recent years, several sections were studied within the Lower Jurassic beds that outcrop along the southern margin of the Ljubljana Moor (Gale, 2014, 2015; Gale & Kelemen 2017). The Staje section correlates well with the Sinemurian Preserje, Tomišelj, Jezero and Zalopate sections, in which the authors describe a gradual opening up of lagoonal sedimentary environments as documented by the increasing presence of bioclastic and later also ooidal limestones (Gale & Kelemen, 2017). The same sedimentary trend continues upwards into Pliensbachian “Podpeč limestone” (microfacies described in detail by Gale, 2015) in which grain-supported facies (pack/grain/rudstone) become even more frequent or even dominate the succession (Buser & Debeljak, 1995; Debeljak & Buser, 1997; Gale, 2014, 2015; Kramar et al., 2015). Sedimentation of the “Podpeč limestone” took place in the lagoon close to ooid shoals that characterized the margin of the Dinaric Carbonate Platform during the

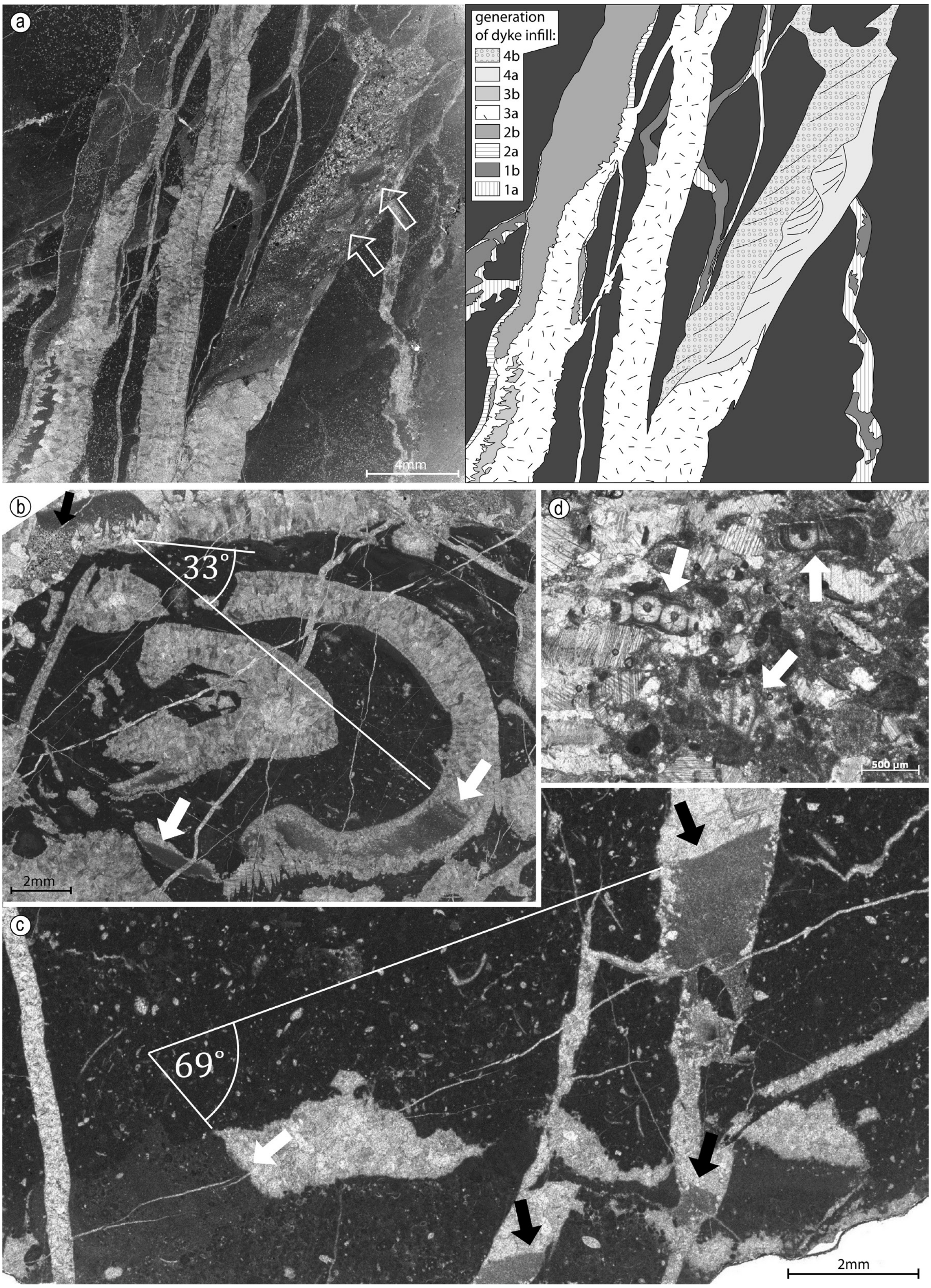

Fig. 10. Microfacies of neptunian dykes.

a) A complex pattern of neptunian dykes. Older dykes are irregular and filled first with cement (1a) and later by fine sediment (1b). The younger phase forms straight, wide-opened fractures filled with thin cement (2a), followed by calcisiltite (2b). The third generation re-opens fractures of previous generations and opens new. It was first filled with coarse-crystalline cement (3a) and small amount of calcisiltite (3b). The last generation re-opens old fractures that fill with sediment, presumably in two generations: the older (4a) shows sliding (indicated by arrows) that occurred during the final opening and refilling (4b) of the fracture (sample 4.8).

b) Difference of 33° in geopetal infilling of dissolved bivalve shell and fenestrae (white arrows) and those of neptunian dykes (black arrow) (sample 1.4).

c) Difference of 69° in geopetal infilling of fenestrae (white arrows) and those of neptunian dykes (black arrows) (sample 5.3).

d) Composition of neptunian dyke: intraclasts, small superficial ooids, pellets, echinoderm plates and other bioclasts with latest Jurassic *Clypeina jurassica* Favre (arrows) (sample 5.4).

Lower Jurassic (Buser & Debeljak, 1995). A similar Lower Jurassic succession is also described from the Kovk section in western Slovenia (Črne & Goričan, 2008) and can be recognized in the lithostratigraphic subdivision that was proposed by Dozet and Strohmenger (2000) and Dozet (2009).

Neptunian dykes: The neptunian dykes from the Staje section show a rather complex relationship between cement and sediment infills, which points to a pulsating opening of the fractures. The nature of infill during each pulse is related to the connection of the fractures to the surface. Cements were closing the fractures during periods of poor connection with the surface or during emersion. Sediment infilled the fractures during the well-established connection of the fractures with the sea bottom. Although these opening pulses could originate during several chronologically distant extensional phases, we propose that these fractures formed inside a relatively short time during the Late Jurassic. This is suggested by (A) *Clypeina jurassica* Favre determined in the sediment of the neptunian dykes, (B) the similar sediment infill of different pulses and (C) a soft deformation inside the older sediment covered by younger sediment.

The neptunian dykes of the Staje section are connected to the middle Late Jurassic tectonic phase that is well expressed on the Dinaric Carbonate Platform. It is seen as a widespread emersion that terminated the growth of the vast barrier reef and is documented in the form of bauxites and horizons of polymict breccias (Buser, 1989; Strohmenger & Dozet, 1990; Dozet, 1994; Dozet et al.,1996; Turnšek, 1997; Vlahović et al., 2005; Buser & Dozet, 2009). The breccia is polygenetic, and is interpreted as karst breccia or talus breccia originating along scarps and is followed by shallow water limestones characterised by *Clypeina jurassica* Favre (Strohmenger & Dozet, 1990; Buser & Dozet, 2009). Reports of neptunian dykes within the Jurassic strata of the Dinaric Carbonate Platform are rare (Otoničar, 2015; Žibret, 2015). On the contrary, they are well known from the northerly Julian Carbonate Platform located today in the Southern Alps (Babić, 1981; Buser, 1996). One of these extensional phases was dated as upper Late Jurassic (Šmuc, 2005; Črne et al., 2007).

The Lower Jurassic beds are covered in the Krim-Mokrec Mountain Range by a succession of Middle Jurassic ooidal limestone strata some several hundred meters thick, followed in the wider region by Upper Jurassic reefal limestone and subsequent lagoonal limestones with C*lypeina jurassica* (Turnšek 1997; Miler & Pavšič, 2008; Buser & Dozet, 2009). The connection of the fractures within Lower Jurassic strata to the upper Upper Jurassic surface/sea bottom is therefore somewhat problematic, especially as no large-scale neptunian dykes have yet been detected within the younger strata. A possible solution arises out of the fact that in the wider surroundings of the Staje area only Lower Jurassic beds outcrop (fig. 1). It is possible that the investigated succession originated already in marginal parts of the platform that are otherwise known to contain a large-scale (Middle) Jurassic gap (Buser & Dozet, 2009; Otoničar, 2015). A specific succession, where the latest Jurassic strata lies directly on Lower Jurassic lagoonal limestones, was recently described in the Avče area in western Slovenia, which represents one of the northernmost (marginal) Jurassic outcrops of the Dinaric Carbonate Platform (Kovač, 2016).

Natural stone: In the case the Roman quarry existed in the selected location near the village of Staje, the stonecutting products that would have come from the quarry would have been composed predominantly of micritic limestone in microfacies, mostly as fossil-poor mudstone or wackestone with two (or more) distinct generations of dissolution voids (F1B microfacies type). Some voids are filled with reddish sediment. This facies could contain parts (laminae, lenses, pockets…) of other facies, such as bioclastic limestone, calcarenite or microbreccia (lithoclastic rudstone). Another possible facies would be bioclastic limestone in the form of various microfacies, but partly-washed packstone with large mollusks is most common (F2C microfacies type). Calcarenites composed either of ooids or aggregate grains are subordinate and occur in generally thinner beds. Their use is less probable, but could be considered more probable in view of their characteristics that make them suitable for stone-cutting. Our field observations show that similar natural stones would have been obtained also from other potential quarries of the wider Staje (Ig) area, as the composition of the succession is monotonous. A thin-section made from the massive outcrop with the "Stari dedec" stela at the entrance of the valley confirms our proposition. It shows that the outcrop is a fenestral (birds-eyes) mudstone (F1B microfacies type). On the margin of the thin section it passes with a sharp, curved contact into intraclastic/pelletal dense wackestone/partly-washed packstone, which generally corresponds to our F1I microfacies type, but additionally contains some anomuran pellets. The later grains were not detected from the Staje section, but are reported from other, Lower Jurassic sections (Gale, 2015) located close by. This helps explain the fact that, despite dense sampling, it is not possible to describe all the microfacies that can be extracted from the studied section, and other varieties can be expected within the frame of the studied sedimentary environment.

Similar natural stones could have been acquired also from quarries of the Podutik area, located just north of Ljubljana. This natural stone is known as "gliničan" and was likely quarried already in Roman times (Ramovš, 1990; in Šašel-Kos, 1997). The Lower Jurassic limestone of the Podutik area represents a time and facies equivalent of the succession studied in the Staje section (Novak, 2003; Vodnik, 2016; Vodnik et al., 2017). Those characteristics that might distinguish the sites may consist in the Late Jurassic neptunian dykes that were detected in the "main wall" of the potential Roman quarry near Staje. Such features were not described from the Podutik area, but reddish and greenish colored veins, i.e. potential neptunian dykes, are reported (Ramovš, 1990; Novak, 2003; Vodnik, 2016, Vodnik et al., 2017), and study of their microfacies would be welcomed in the future.

Conclusions

Geomorphological study and field observations indicate that the Roman quarry in the Staje area could potentially be located in the valley running SE of the village. The section logged across the wall at the SW bank of the valley shows that the studied succession is composed of micritic limestone, subordinate bioclastic limestone and rare calcarenite and limestone microbreccia. Most common microfacies are mud/wackestone with several generations of dissolutions voids (often with geopetal fill) and partly-washed packstone with large mollusks. Calcarenite is pack/grainstone, dominated either by aggregate grains or ooids.

The sedimentary environment was restricted to an open marine lagoon with repeating subaerial exposure. High-energy events, which are indicated by sandy facies (ooidal pack/grainstone, aggregate grains pack/grainstone, bioclastic grainstone) and lumachella (bioclastic rudstone), occasionally interrupted the "quiet" lagoonal conditions. The studied section is Sinemurian in age and fits well within the Hettangian to Pliensbachian opening of the sedimentary environment from intertidal flats to a differentiated lagoon from the previously described northern part of the Dinaric Carbonate Platform.

The section is characterized by neptunian dykes that reveal a pulsating opening of the fractures but which were presumably formed within a relatively short time in the Late Jurassic, as evidenced by *Clypeina jurassica* Favre determined in the sediment fill. The neptunian dykes could be distinguishing characteristics of the Staje succession, allowing for a distinction from the potential Roman quarry site in Podutik, just north of Ljubljana, that represents a time and facies equivalent succession. However, an additional study of the reddish and green-coloured "veins" that are reported from the Podutik site are needed to confirm our proposal.

Acknowledgment

This research was financially supported by the Slovenian Research Agency (research core funding No. P1-0195(B) and No. P1-0011). We sincerely thank Rajka Radojčić for determination of *Clypeina jurassica* Favre. Anonymous reviewers are acknowledged for their thorough review of the manuscript, and Ema Hrovatin for preparation of thin sections.

References

Babić, L. 1981: The origin of "Krn breccia" and the role of the Krn area in the Upper Triassic and Jurassic history of the Julian Alps. Vesnik Zavoda geol. Geofiz. istraživanja NR Srbije, 38/39: 59–87.

BouDagher-Fadel, M. & Bosence, D. W. J. 2007: Early Jurassic benthic foraminiferal diversification and biozones in shallow-marine carbonates of Western Tethys. Senck. Lethaea, 87: 1-39.

Buser, S. 1968: Osnovna geološka karta SFRJ, list Ribnica. Zvezni geološki zavod Jugoslavije, Beograd.

Buser, S. 1989: Development of the Dinaric and the Julian carbonate platforms and of the intermediate Slovenian Basin NW Yugoslavia. Memor. Soc. Geol. Ital., 40: 313–320.

Buser, S. 1996: Geology of Western Slovenia and its paleogeographic evolution. In: Drobne, K., Goričan, Š. & Kotnik, J. (eds.): The role of impact processes in the geological and biological evolution of planet earth. Abstracts from Int. Symp., Postojna, Slovenia, September 1996, 111–123.

Buser, S., Grad, K. & Pleničar, M. 1967: Osnovna geološka karta SFRJ, list Postojna. Zvezni geološki zavod Jugoslavije, Beograd.

Buser, S. & Debeljak, I. 1995: Lower Jurassic beds with bivalves in South Slovenia. Geologija, 37/38: 23–62, doi: https://doi.org/10.5474/geologija.1995.001.

Buser, S. & Dozet, S. 2009: Jura - Jurassic. In: Pleničar, M., Ogorelec, B. & Novak, M. (eds.): Geologija Slovenije = The geology of Slovenia. Geološki zavod Slovenije, Ljubljana: 215-254.

Celarc, B. 2004: Problems of the Cordevolian limestone and dolomite in the Slovenian part of the Southern Alps. Geologija, 47: 139-149, doi: https://doi.org/10.5474/geologija.2004.011

Celarc, B. 2008: Carnian bauxite horizon on the Kopitov grič near Borovnica (Slovenia) - is there a „forgotten" stratigraphic gap in its footwall? Geologija, 51/2: 147-152, doi: https://doi.org/10.5474/geologija.2008.015

Chiocchini, M., Farinacci, A., Mancinella, A., Molinari, V. & Potetti, M. 1994: Foraminiferal, dasycladacean and calpionellid biostratigraphy of the Mesozoic carbonates of the Central Apennines Italy. In: Biostratigraphy of the Central Italy. Studi Geol. Camerti, Roma, 9-130.

Črne, A. E., Šmuc, A. & Skaberne, D. 2007: Jurassic neptunian dikes at Mt Mangart (Julian Alps, NW Slovenia). Facies, 53: 249-265, doi: https://doi.org/10.1007/s10347-007-0102-8 .

Črne, A. E. & Goričan, Š. 2008: The Dinaric Carbonate Platform margin in the Early Jurassic: a comparison between successions in Slovenia and Montenegro. Boll. Soc. Geol. It. - Ital. J. Geosci., 127: 389–405.

Debeljak, I. & Buser, S. 1997: Lithiotid bivalves in Slovenia and their mode of life. Geologija, 40: 11–64, doi: https://doi.org/10.5474/geologija.1997.001.

Dozet, S. 1994: Malmian bauxites at Kočevska Reka and Kočevje. RMZ-Materials and Geoenvironment, 41: 215-219.

Dozet, S. 2009: Lower Jurassic carbonate succession between Predole and Mlačevo, Central Slovenia. RMZ – Materials and Geoenvironment, 56: 164–193.

Dozet, S. 2014: Apneničarstvo na južnem robu Ljubljanskega barja – Apnenice na Ižanskem. Mostiščar. 20/5: 18-19.

Dozet, S. & Strohmenger, C. 2000: Podbukovje Formation, Central Slovenia. Geologija, 43/2: 197–212, doi: https://doi.org/10.5474/geologija.2000.014.

Dozet, S., Mišič M. & Žuža, T. 1996: Malm Bauxite Occurences in Logatec, Nanos and Kočevje area. RMZ-materials and geoenvironment, 43: 23-35.

Djurić, B. & Rižnar, I. 2017: Kamen Emone = The rocks for Emona. In: Vičič, B. & Županek, B. (eds.): Emona MM: urbanizacija prostora - nastanek mesta = urbanisation of space - beginning of a town. Zavod za varstvo kulturne dediščine Slovenije: Mestni muzej, Muzej in galerije mesta Ljubljane: 121-144.

Flügel, E. 2004: Mikrofacies of Carbonate Rocks. Springer Verlag, Berlin: 976 p.

Gale, L. 2014: Lower Jurassic foraminiferal biostratigraphy of Podpeč limestone External Dinarides, Slovenia. Geologija, 57/2: 119–146, doi: https://doi.org/10.5474/geologija.2014.011.

Gale, L. 2015: Microfacies characteristics of the Lower Jurassic lithiotid limestone from Northern Adriatic Carbonate Platform Central Slovenia. Geologija, 58/2: 121–138, doi: https://doi.org/10.5474/geologija.2015.010.

Gale, L. & Kelemen, M. 2017: Early Jurassic foraminiferal assemblages in platform carbonates of Mt. Krim, central Slovenia. Geologija, 60: 99-115, doi: https://doi.org/10.5474/geologija.2017.008.

Kovač, A. 2016: Biostratigrafija in sedimentologija srednjejurskih in spodnjekrednih plasti v dolini Soče pri HE Doblar. Diplomsko delo, Univerza v Ljubljani, Ljubljana: 61 p.

Kramar, S., Bedjanič, M., Mirtič, B., Mladenovič, A., Rožič, B., Skaberne, D., Gutman, M., Zupančič, N. & Cooper, B. J. 2015: Podpeč limestone: a heritage stone from Slovenia. In: Pereira, D. et al. (eds.): Global heritage stone: towards international recognition of building and ornamental stones, London, 219–231, doi: http://dx.doi.org/10.1144/SP407.2.

Miler, M. & Pavšič, J. 2008: Triassic and Jurassic beds in Krim Mountain area Slovenija = Triasne in jurske plasti na območju Krima. Geologija, 51/1: 87–99, doi: https://doi.org/10.5474/geologija.2008.010.

Mušič, B. 1990: Razvoj zgornjepermijskih in spodnjetriasnih plasti pri Višnji gori in Skopačniku pri Želimljah. – Neobjavljena diplomska naloga / Unpublished BA thesis. Oddelek za geologijo, Naravoslovnotehniška fakulteta Univerze v Ljubljani.

Novak, M. 2003: Zgornjetriasne in spodnjejurske plasti na območju Podutika pri Ljubljani - Upper Triassic and Lower Jurassic beds in the Podutik area near Ljubljana (Slovenia). Geologija, 46/1: 65-74, doi: https://doi.org/10.5474/geologija.2003.004.

Otoničar, B. 2015: Evolucija severovzhodnega obrobja Jadranske karbonatne platforme med zgornjim triasom in zgornjo juro Dolenjska, JV Slovenija:. In: Rožič, B. (ed.): Razprave, poročila = Treatises, reports, 22. posvetovanje slovenskih geologov = 22nd Meeting of Slovenian Geologists, Ljubljana, november 2015, Geološki zbornik, 23: Ljubljana: Univerza v Ljubljani, NTF, Oddelek za geologijo, 23: 147-150.

Placer, L. 1999: Contribution to the macrotectonic subdivision of the border region between Southern Alps and External Dinarides. Geologija, 41: 223-255, doi: https://doi.org/10.5474/geologija.1998.013.

Placer, L. 2008: Principles of the tectonic subdivision of Slovenia. Geologija, 51: 205-217, doi: https://doi.org/10.5474/geologija.2008.02.1

Ragolič, A. 2016: The funerary stele of Petto from Ig. Arheološki vestnik, 67: 277-296.

Ramovš, A. 1990: Gliničan od Emone do danes. Odsek za geologijo, VTOZD Montanistika, Fakulteta za naravoslovje in tehnologijo, Ljubljana.

Ramovš, A. 2000: Podpeški in črni ter pisani lesnobrdski apnenec skozi čas. Mineral, Ljubljana.

Senowbari-Daryan, B., Bucur, I. & Abate, B. 1994: Upper Jurassic calcareous algae from the Madonie Mountains, Sicily. Beitr. Paläont., 19: 227-259.

Strohmenger, C. & Dozet, S. 1990: Stratigraphy and geochemistry of Jurassic carbonate rocks from Suha krajina and Mala gora mountain (Southern Slovenia). Geologija, 33: 315-351, doi: https://doi.org/10.5474/geologija.1990.008.

Šašel, J. 1959: Prispevki za zgodovino rimskega Iga. Kronika, Časopis za slovensko krajevno zgodovino, 7: 117–123.

Šašel Kos, M. 1997: The Roman Inscriptions in the National Museum of Slovenia / Lapidarij Narodnega muzeja Slovenije. Situla: razprave Narodnega muzeja Slovenije = dissertationes Musei nationalis Sloveniae, 35: 541 p.

Šašel Kos, M. 2009: Ig – a rural settlement on the southern edge of the Ljubljansko barje. In: Turk, P., Istenič, J., Knific, T. & Nabergoj, T. (eds.): The Ljubljanica – a River and its Past. Ljubljana: 108–111.

Šmuc, A. 2005: Jurassic and Cretaceous Stratigraphy and Sedimentary Evolution of the Julian Alps, NW Slovenia. Založba ZRC, Ljubljana: 98 p.

Turnšek, D. 1997: Mezosoic Corals of Slovenia. Založba ZRC, Ljubljana: 512 p.

Velić, I. 2007: Stratigraphy and palaeobiogeography of Mesozoic benthic Foraminifera of the Karst Dinarides SE Europe. Geologia Croatica, 60: 1-113.

Velušček, A. 2004: Past and present lake-dwelling studies in Slovenia. Ljubljansko barje the Ljubljana Marsh: In: Menotti, F. (ed.): Living on the Lake in Prehistoric Europe. 150 years of Lake-dwelling Research, London, New York: 69–82.

Velušček, A. 2010: Koliščarji: o koliščarjih in koliščarski kulturi Ljubljanskega barja. Založba ZRC, Ljubljana: 109 p.

Veranič, D. & Repanšek, L. 2016: Rimski kamniti spomeniki iz cerkve sv. Janeza Krstnika v Podkraju pri Tomišlju = Roman stone monuments in the Church of St. John the Baptist in Podkraj near Tomišelj. Arheološki vestnik, 67: 297–320.

Vlahović, I., Tišljar, J., Velić, I. & Matičec, D. 2005: Evolution of the Adriatic Carbonate Platform: Paleogeography, main events and depositional dynamics. Paleogeography, Paleoclimatology, Paleoecology, 220: 333-360, doi: https://doi.org/10.1016/j.palaeo.2005.01.011.

Vodnik, P. 2016: Litološke značilnosti spodnjejurskega apnenca pri Podutiku in Kamni Gorici ter primerjava z artefakti iz časa Emone: diplomsko delo = Lithological characteristics of Lower Jurrasic limestone at Podutik and Kamna Gorica Central Slovenia: and its comparison with artefacts from Roman Emona: diploma work. Ljubljana: 49 p.

Vodnik, P., Djurić, B. & Gale, L. 2017: Vrednotenje možnosti lokacije rimskega kamnoloma v Podutiku na podlagi sedimentološke analize. In: Rožič, B. (ed.): Razprave, poročila = Treatises, reports, 23. posvetovanje slovenskih geologov = 23rd Meeting of Slovenian Geologists, Geološki zbornik, 24: 183-185.

Vuga, D. 2000a: Stari Dedec pri Stajah: lapis sepulcralis gentis Laepiae. Kras, 42: 10-11.

Vuga, D. 2000b: Ižanski lapidarij. Rodna gruda. Revija za Slovence po svetu. 47/7: 48.

Žibret, L. 2015: Kinematski in paleonapetostni razvoj NW-SE usmerjenih dinarskih prelomov v severozahodnih zunanjih Dinaridih: doktorska disertacija = Kinematic and paleostress evolution of the NW-SE trending Dinaric faults in the northwestern External Dinarides. PhD Thesis, University of Ljubljana, Ljubljana: 84 p.

Žvab Rožič, P., Gale, L. & Rožič, B. 2016: Rock analysis of Roman tombstones from Podkraj and Ig near Ljubljana. Arheološki vestnik, 67: 359-369.